NPS67-78-010

NAVAL POSTGRADUATE SCHOOL

Monterey, California

FIN-OPENING DYNAMICS FOR AN 8-INCH GUN LAUNCHED EXTENDED-RANGE GUIDED PROJECTILE

Louis V. Schmidt

December 1978

Approved for public release; distribution unlimited

Prepared for:
Naval Weapons Center
China Lake, CA 93555

NAVAL POSTGRADUATE SCHOOL

Monterey, California

Rear Admiral T. F. Dedman
Superintendent

Jack R. Borsting
Provost

The work reported herein was supported by the Naval Weapons Center, China Lake, California.

This report was prepared by:

Louis V. Schmidt

LOUIS V. SCHMIDT
Professor of Aeronautics

Reviewed by:

M. F. Platzer

M. F. PLATZER, Chairman
Department of Aeronautics

Released by:

William M. Tolles

W. M. TOLLES
Dean of Research

UNCLASSIFIED
SECURITY CLASSIFICATION OF THIS PAGE (When Data Entered)

REPORT DOCUMENTATION PAGE

READ INSTRUCTIONS BEFORE COMPLETING FORM

1. REPORT NUMBER: NPS67-78-0k0
2. GOVT ACCESSION NO.
3. RECIPIENT'S CATALOG NUMBER

4. TITLE (and Subtitle): FIN-OPENING DYNAMICS FOR AN 8-INCH GUN LAUNCHED EXTENDED-RANGE GUIDED PROJECTILE,
5. TYPE OF REPORT & PERIOD COVERED: Final Rept. July 1976 - December 1978
6. PERFORMING ORG. REPORT NUMBER

7. AUTHOR(s): Louis V. Schmidt
8. CONTRACT OR GRANT NUMBER(s): N60530-76-WR-30186

9. PERFORMING ORGANIZATION NAME AND ADDRESS: Naval Postgraduate School, Department of Aeronautics, Monterey, CA 93940
10. PROGRAM ELEMENT, PROJECT, TASK AREA & WORK UNIT NUMBERS: 63368N

11. CONTROLLING OFFICE NAME AND ADDRESS: Naval Weapons Center, Attn: Code 3272, China Lake, CA 93555
12. REPORT DATE: 11 December 1978
13. NUMBER OF PAGES: 73

14. MONITORING AGENCY NAME & ADDRESS(if different from Controlling Office): NAVP
15. SECURITY CLASS. (of this report): UNCLASSIFIED
15a. DECLASSIFICATION/DOWNGRADING SCHEDULE

16. DISTRIBUTION STATEMENT (of this Report)

Approved for public release; distribution unlimited

17. DISTRIBUTION STATEMENT (of the abstract entered in Block 20, if different from Report)

NPS67-78-010

18. SUPPLEMENTARY NOTES

19. KEY WORDS (Continue on reverse side if necessary and identify by block number)

20. ABSTRACT (Continue on reverse side if necessary and identify by block number)

The fin-opening dynamics for an 8-inch Gun Launched Extended-Range Guided Projectile (ERGP) were analyzed during the typical 20 to 30 millisecond time span immediately after the missile departed the gun barrel. Lagrange's equations were used to develop a set of governing dynamic relationships using four generalized coordinates including missile roll angle, fin-opening angle and fin bending and torsion deflections. The latter two coordinates provided an elastic representation for accommodating the fin's transient response during the fin-opening process.

DD FORM 1 JAN 73 1473 EDITION OF 1 NOV 65 IS OBSOLETE
S/N 0102-014-6601

UNCLASSIFIED
SECURITY CLASSIFICATION OF THIS PAGE (When Data Entered)

Sufficient details were provided in the report so that the analytic model could be modified for other missile and fin configurations, including the addition of more fin bending degrees of freedom.

Comparison was made between the analysis results and a limited amount of experimental evidence. Agreement was reached with fin-opening times and an indirect conclusion was reached that initial fin-opening angle rates were in the range of 35 to 50 radians per second.

The fin elastic response was shown to be dependent primarily upon the fin bending mode. Peak stress encounters by the fin root beyond yield could be avoided by configuring the ERGP obturator rings to control initial missile roll rates to less than 15 revolutions per second. This latter point is important since local yielding of the fins by excessive bending stresses, incurred during launch, can adversely effect the trajectory dynamics by contributing to the presence of a residual roll rate.

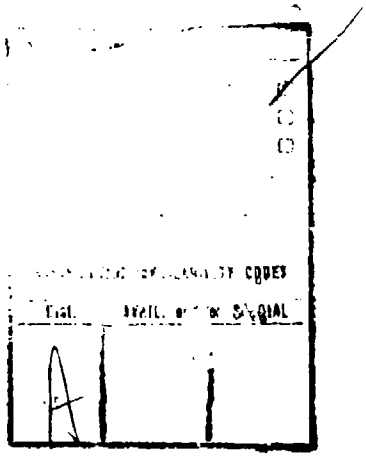

TABLE OF CONTENTS

LIST OF FIGURES

LIST OF TABLES

LIST OF SYMBOLS AND ABBREVIATIONS

A	Matrix array of inertial influence coeffs., eqn. 4
c.g.	Center of gravity
E	Young's modulus of elasticity
ERGP	Extended Range Guided Projectile
$\mathcal{F}$	Impulse, translational form
g	Column vector, eqn. 4
G	Shear modulus
.GE.	Greater than or equal to
Hz	Hertz, 1/second
I	Mass moment of inertia, usually subscripted
K	Spring constant, usually subscripted
.LT.	Less than
M	Mass, usually subscripted
MS	Millisecond
NWC	Naval Weapons Center
q	Column vector of generalized coordinates, eqn. 4
R_o	Radial distance of fin pivot to GLGP centerline
T	Kinetic energy
T_{60}	Time for fin deployment to 60 degrees
v	Translational velocity, usually subscripted
V	potential energy
x	Rectilinear coordinate
α	Fin bending coordinate
β	Fin torsion coordinate
Δ	Increment notation when used as a prefix
Θ	Fin opening angle

ϕ	Missile roll angle
ρ	Mass density
σ	Tensile stress due to bending
$\dot{(\ )}$	Time derivative, d( )/dt
$(\ )_{xx}$	Variable oriented by subscript "xx" "xx" = 1, 2, or 3: Reference axes "xx" = MAX: Maximum value
[ ]	Square matrix array
{ }	Column vector array

I. INTRODUCTION

A gun-launched extended-range guided projectile (ERGP) is confronted with a transitional problem in that it is launched from a rifle barrel as a rotating bullet-shaped member and must then convert into an almost non-rotating finned missile before firing a self-contained rocket propulsion system. The resident guidance system places a constraint upon the roll rate residual of approximately +/- one (1) revolution per second after the fins have opened and provided roll damping. Since the residual roll rate of the projectile is an open-loop situation (i.e., no roll control is provided), there are two principal difficulties associated with meeting a design goal on the residual roll rate. One problem is relative to fin alignment, with the residual roll rate tolerance requiring the fins to be aligned with the freestream to a small fraction of a degree. Another problem concerns the question whether fin-opening dynamics introduces stresses into the fin such that structural yielding occurs thereby providing a separate source for fin angular misalignment, and as a matter of fact, possibly negating the time-consuming efforts spent initially in fin alignment.

The case considered in this report will be the development of fin-opening dynamics for an eight-inch ERGP with a six fin configuration. Although the muzzle velocity of the ERGP is fairly well defined from the typical 40 millisecond acceleration period in the gun barrel, the initial condition upon free-flight roll rate is a variable with maximum values being on the order of 30 revolutions per second prior to fin opening. The initial, fin retracted roll rate is dependent upon the configuration of the obturator rings, which are installed on the ERGP to act as slip rings between the rifle barrel and the missile. The obturator rings go through an engraving process with the rifling, and it is the relative slippage between the rings and the missile which prevents a complete transfer of angular roll momentum during the initial firing process.

The ERGP missile may be assumed as having a constant velocity along its axis of symmetry while conserving angular momentum during the fin-opening process. The dissipative action of the fins upon the roll rate, due to aerodynamic damping in roll, is present to some extent during fin opening but will be neglected since the opening times occur much faster than roll damping time constants; e.g., 0.030 seconds vs. 0.30 seconds respectively for a typical situation.

Although not well defined in magnitude, it is possible that the retracted fins may have an initial condition of opening rate due to an impulse transfer either from the release of the fin latch block or from the gun barrel gas dynamics. Both of these influences are unknown quantities that may occur in varying degrees. Another concern relates to the actual fin structural dynamics, and a question to be addressed concerns whether a fin torsion or bending mode might be significantly excited during the opening and hence provide a magnification of fin stresses. Since the actual environment of the ERSP during launch may be conservatively described as "severe", the principal source of flight data to answer the aforementioned concerns has been photographic in nature.

It is the purpose of the studies described herein to develop equations of motion for fin-opening dynamics under the assumption of angular momentum conservation such that time histories may be obtained for the opening process with various initial conditions of roll rate and fin opening rate for both rigid and elastic fins. From computer solutions of these equations of motion, it would be hoped that some conclusions might be reached relative to fin stress time histories in order to provide a better insight into the overall problem that is loosely categorized under the title of "fin-opening dynamics".

II. THEORY

The development of the relations describing fin-opening dynamics is quite easy to follow when one employs the energy approaches that are implicit in the Lagrange's equation technique; e.g., Goldstein, Ref. 1. The generalized coordinates were chosen such that the rigid system dynamics were described by the missile rotational angle, ϕ, and the fin opening angle, θ. Fin elasticity was modeled by the fundamental bending and torsion modes using a simple pendulum analogy where bending and torsion deformations were expressed by the coordinates α and β respectively. The pendulum model was referenced to the fin base. Figures 1 and 2 show the coordinate systems.

Fin geometry is illustrated on Fig. 3 in accord with Ref. 2. Estimated values locating the center of gravity of the complete fin and respective mass moments of inertia were used for the rigid fin model. When fin elasticity was modeled (a selectable option), the mass and inertial properties were broken down to considerations of fin base and fin blade elements respectively. Table I tabulates the values used for both the rigid and elastic fin analyses.

One may conceptually visualize a refined or improved finite element elastic model using the fin segmented into a four degree of freedom (d.o.f.) system as sketched in Fig. 4. Adding more degrees of freedom will improve the elastic modeling, but in exchange, the equations will become more complex. Since the stiffness values for the pendulum model arise from previous dynamic calculations made in a stationary frame of reference, one must recognize that the bending and torsional excitations in time history calculations represent an approximation much in the sense of using Galerkin's method in aeroelastic calculations where wind-off modes are used to develop the wind-on modes when seeking in-flight stability boundaries.

A. Equations of Motion:

In terms of the generalized coordinates ϕ, θ, α and β, the kinetic and potential energies of the missile may be established. The kinetic and potential energy, T and V respectively, may be functionally recognized as:

$$T = T(\phi, \theta, \alpha, \beta, \dot{\phi}, \dot{\theta}, \dot{\alpha}, \dot{\beta}, t) \qquad \ldots(1)$$

and

$$V = V(\phi, \theta, \alpha, \beta, t) \qquad \ldots(2)$$

TABLE I

Mass and Inertia Properties

ERGP (w/o fins):
$I = 9.859$ lb-in-sec^2
(estimated about missile axis of symmetry)

Fin (one of six):

a. Mass: $M_B = 0.001407$ lb-sec^2-in^{-1}

$M_F = 0.006134$ lb-sec^2-in^{-1}

$M = 0.007541$ lb-sec^2-in^{-1} (total value)

b. Location of c.g. in Fin Coords. ($x_2 = 0$):

Base: $x_{1B} = -0.140$ in.

$x_{3B} = +0.801$ in.

Fin: $x_{1F} = -0.918$ in.

$x_{3F} = +6.231$ in.

Total: $x_1 = -0.774$ in.

$x_3 = +5.225$ in.

$R_o = 2.380$ in. (fin pivot-to-ERGP centerline)

c. Mass Moments of Inertia:

Total fin relative to total fin c.g. location

$I_1 = 0.00742$ lb-in-sec^2

$I_2 = 0.00358$ lb-in-sec^2

$I_3 = 0.00633$ lb-in-sec^2

Fin (excluding base) relative to fin c.g. location

$I_{1F} = 0.00329$ lb-in-sec^2

$I_{2F} = 0.00821$ lb-in-sec^2

$I_{3F} = 0.00492$ lb-in-sec^2

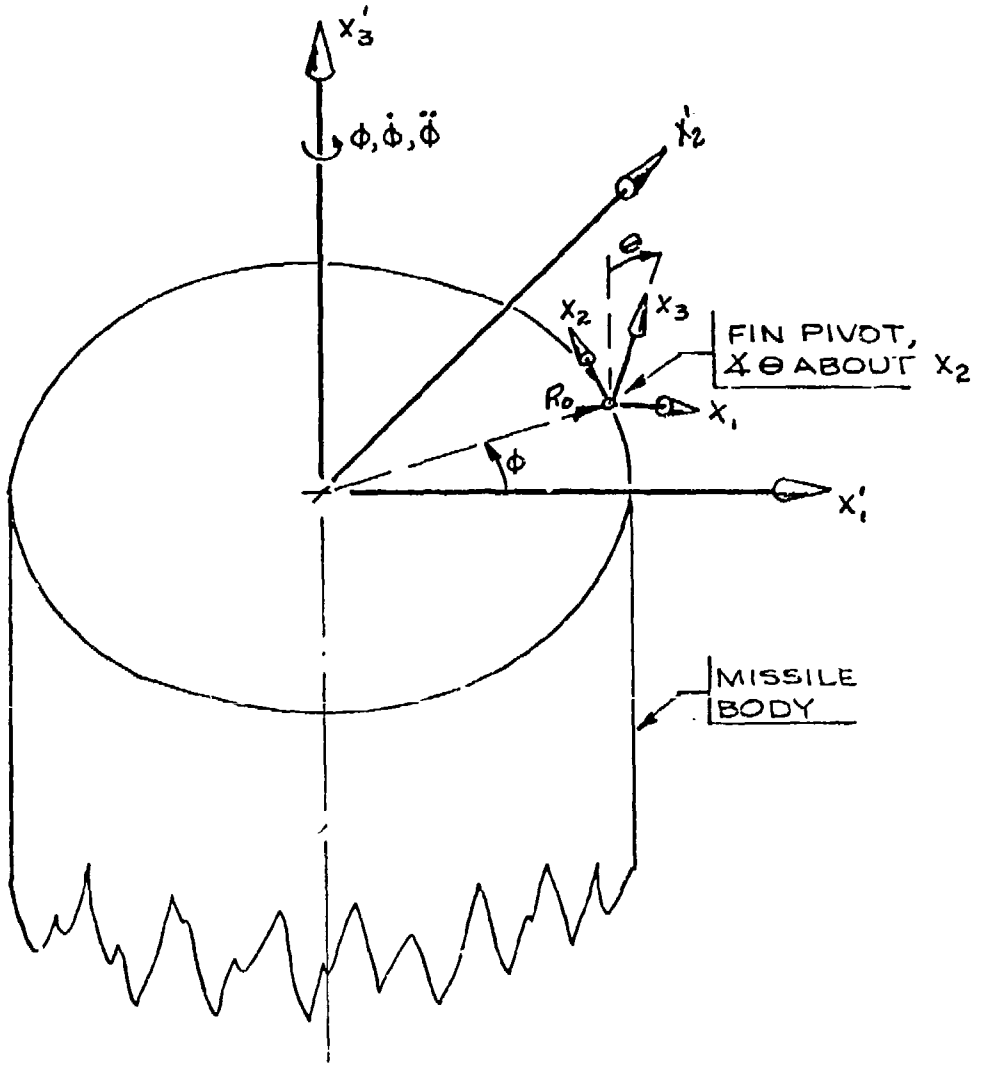

INERTIAL COORDS. : X_1', X_2, X_3'
FIN COORDS : X_1, X_2, X_3
GENRLZD. COORDS : ϕ, θ

FIG. 1: MISSILE COORDINATE SYSTEM

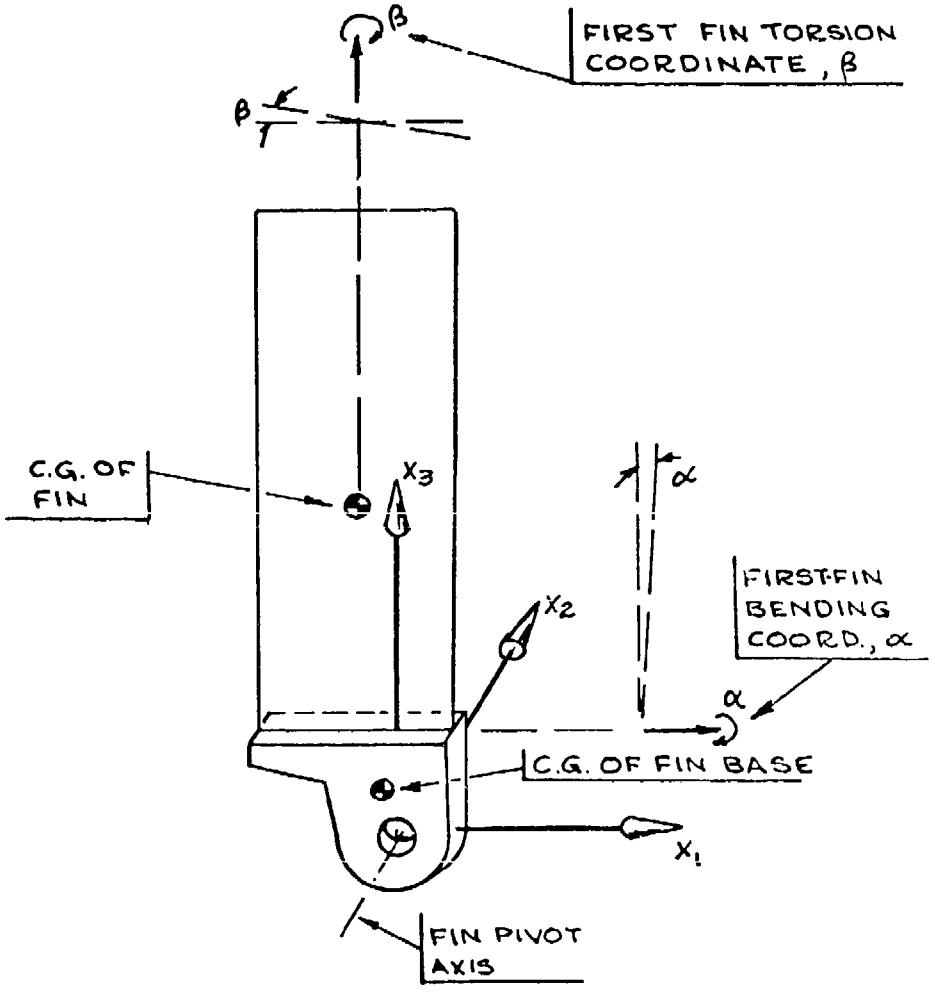

FIG. 2: ELASTIC FIN COORDINATES

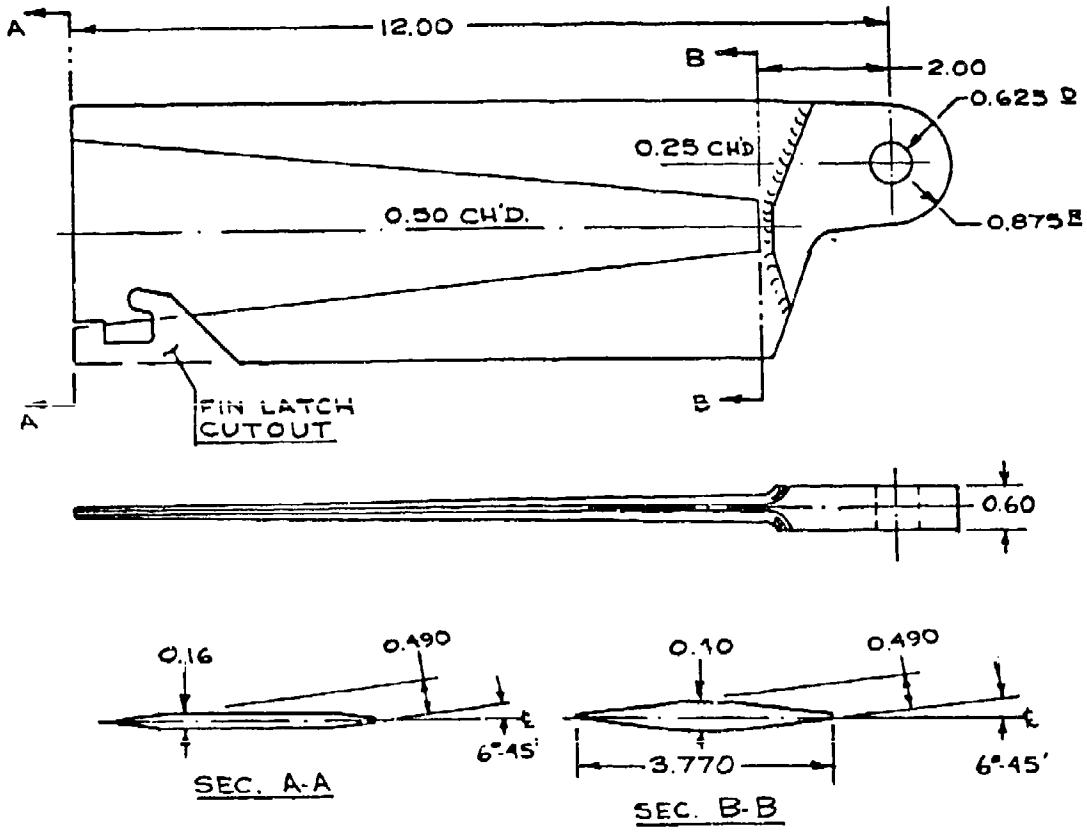

REF.: NWC DWG. SK4503920

FIG. 3: FIN GEOMETRY

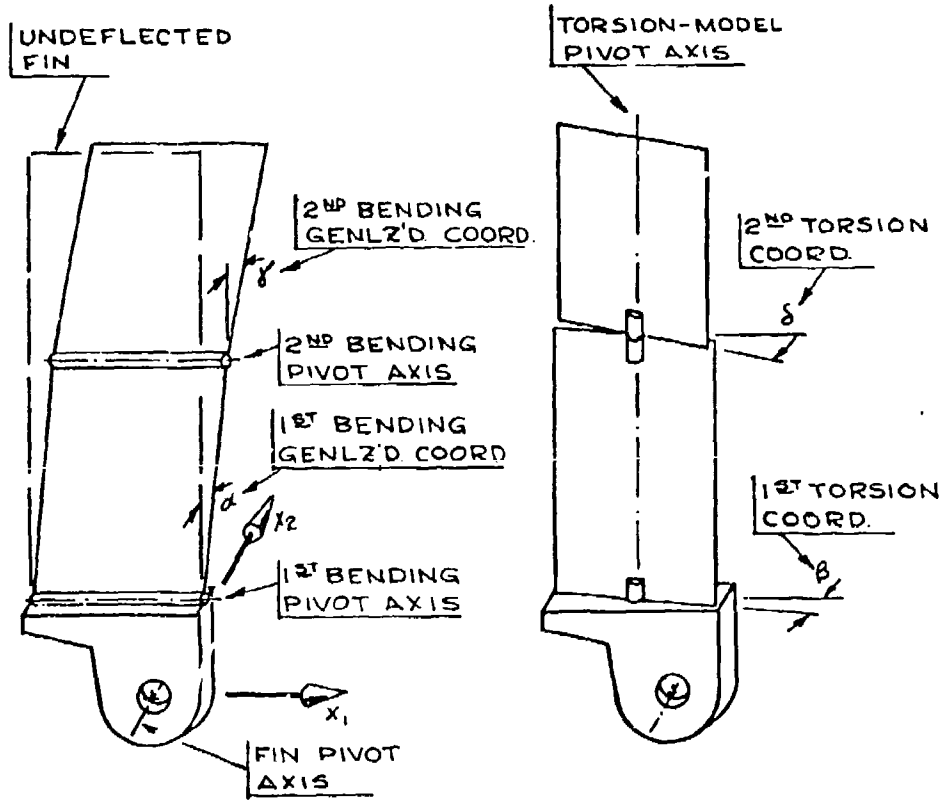

A: TWO BENDING DEGREES-OF-FREEDOM

B: TWO TORSION DEGREES-OF-FREEDOM

FIG. 4: FIN ELASTICITY MODELING

For the freely rotating missile, the roll angle, Φ, will not in general involve potential energy storage. The fin opening angle, Θ, will involve potential energy storage upon impact with the crushable limit stops. The fin bending and torsion elastic model using the simple pendulum as an approximation to the fundamental modes will introduce potential energy due to elastic deformations in α and β.

The application of Lagrange's method to the above relations for kinetic and potential energy allows us to express the equations as:

$$\frac{d}{dt}\left(\frac{\partial T}{\partial \dot{q}_i}\right) - \frac{\partial T}{\partial q_i} + \frac{\partial V}{\partial q_i} = 0 \quad (i=1, 2, 3 \text{ and } 4)$$

for $q_1 = \Phi$, $q_2 = \Theta$ ...(3)

$q_3 = \alpha$, $q_4 = \beta$

The above equations correspond to four angular momentum conservation relations with coordinates tailored for the problem. Since some of the coordinates are in a moving frame of reference, the equations include terms described as Coriolis type accelerations. Their presence is automatically included in the Lagrangian development. In the theory of small vibrations, the derivative of kinetic energy with respect to the generalized coordinate, $\partial T/\partial q_i$, is omitted as a consequence of linearization. Such is not the case in the nonlinear relations considered here since the $q_1 = \Phi$ and $q_2 = \Theta$ deformations were not small perturbations. The right hand side of eqn. 3 being equal to zero implies that the system was not considered with an external forcing function. However, solutions for the set of second order, nonlinear homogeneous differential equations will depend upon the prescribed initial conditions in q_i and $\dot{q}_i$.

B. Solution Procedure:

The terms involved in eqn. 3 are developed in Appendix A. The solution procedure for numerical analysis involves expressing the equations in matrix form as:

$$A\,\ddot{q} = g \qquad \text{...(4)}$$

where the square matrix A introduces the inertial properties of the system with a time dependent, nonlinear coupling relative to the fin-opening angle, Θ, using trigonometric relations. The matrix A is not diagonal, hence convenient solutions are not readily obvious. The column matrix g involves the elastic moments due to fin bending and torsion. It also involves cross product terms of angular rates in an interactive manner in addition to a trigonometric dependence

upon fin opening angle.

Numerical solutions of eqn. 4 were obtained using the IBM 360-67 digital computer located at the W.R. Church Computation Center, Naval Postgraduate School. The solution procedure was based upon a fourth order Runge-Kutta integration procedure using the features of the Continuous System Modeling Program (CSMP) as described by Speckhart and Green, Ref. 3. Software details are given in Appendices B and C.

The A matrix in eqn. 4, although time dependent, is nonsingular at any given instant of time based upon physical arguments. Therefore, each application of the Runge-Kutta integration scheme required uncoupling the highest order time derivatives in eqn. 4 by performing an interim step; i.e., at any time t, determine:

$$\ddot{q}(t) = A(q,t)^{-1}\, g(q, \dot{q}, t) \qquad \ldots(\ 5\ )$$

Successive applications of the algorithms available by the CSMP procedure provided straightforward time history listings of q and $\dot{q}$. An output sample is given in Appendix D.

Since the CSMP procedure allows the use of FORTRAN type logic expressions, it was relatively simple to provide a physical modeling of the crushing action for a representation of the fin impacting into the limit travel stops. Although the use of another computational language may appear foreboding as a usable tool, it was the feeling of the author that the documentation, Ref. 3, and principles involved in CSMP were so well expressed that anyone moderately familiar with computational methods would have little difficulty applying the technique.

C. Fin Modes:

The desire to include the first few vibration modes of the fin into the time history dynamic model led to a search for a finite element representation of the fin. Fortunately, a finite element model consisting of 77 plate elements with 90 node points was available to represent the fin as a thin plate, and the required information was provided by Payne, Ref. 4. A planview sketch of the finite element model may be seen on Fig. 5. The inertial and stiffness properties of the fin were based upon:

ρ = Mass density = 7.303×10^{-4} lb-sec^2-in^{-4}

E = Young's modulus = $30.77 \times 10^{+6}$ psi

G = Shear modulus = $11.20 \times 10^{+6}$ psi

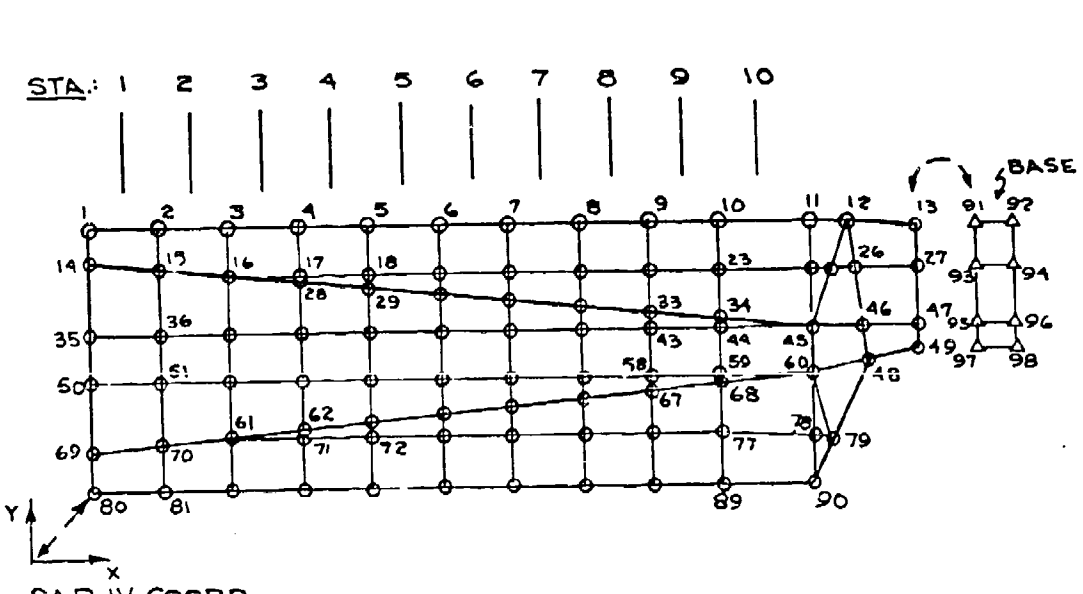

FIG.5: PLATE ELEMENT LAYOUT FOR FIN

The fin element model was used as data input to a structural analysis program, SAP IV, available at the NPS computer center using the instructions as documented by Bathe, Wilson and Peterson, Ref. 5. The first three modes were identified as first and second bending and first torsion at characteristic frequencies of 89.4, 411.4 and 517.0 Hz respectively. Sketches of the mode shapes may be seen on Figs. 6 to 8.

The fin was excited on a shaker table available in the Department of Aeronautics, NPS for the purpose of verifying the modal frequencies and modes. The actual mounting of the fin onto the table was by means of clamping the fin base between two - 1/2 inch thick aluminum plates such that the fin was harmonically excited by lateral motion of the base; i.e., oscillations normal to the fin chord plane. Measured modal frequencies were 81.3, 355 and 430 Hz with the modes identified by observing the nodal lines using salt crystals. The ordering of the mode shapes and the location of the node lines were in accord with the computer results. The lowered values of the characteristic frequencies as compared to the theoretical values may be attributed to the clamping mechanism being elastic.

The alternate wedge shaped fin (Ref. 6), Fig. 9, was also vibrated on the shaker table. Natural frequencies were experimentally observed at 84, 354 and 422 Hz for first and second bending and first torsion modes respectively. The proximity of the experimental modal frequencies to those of the diamond shaped fin would suggest using approximately the same theoretical values for the fin dynamic analysis.

Equivalent pendulum model stiffness values were estimated in the fin-dynamic analysis based upon the fin inertia values of Table I with an assumed pendulum pivot point in the neighborhood of the fin base. Based upon this model, equivalent spring rates for approximating the first bending and torsion modes were (respectively):

$$K_{\alpha} = 1.681 \times 10+4 \text{ in-lb/rad}$$

$$K_{\beta} = 5.190 \times 10+4 \text{ in-lb/rad}$$

The first and second bending modes could be approximated by a double pendulum analogy as a further refinement to the initial analysis. Based upon a knowledge of the node line for the second bending mode and the corresponding frequencies for first and second bending, an intuitive form of parameter identification could be used to develop the double pendulum model with respect to both inertia and spring stiffness traits. This type of a refinement was not attempted in the dynamic model used in the following studies

with the primary reason being that the analysis was an exploratory effort to evaluate the importance of fin elasticity upon fin-opening behavior. The initial considerations of only the fundamental modes should be viewed as a starting point for subsequent analysis refinements.

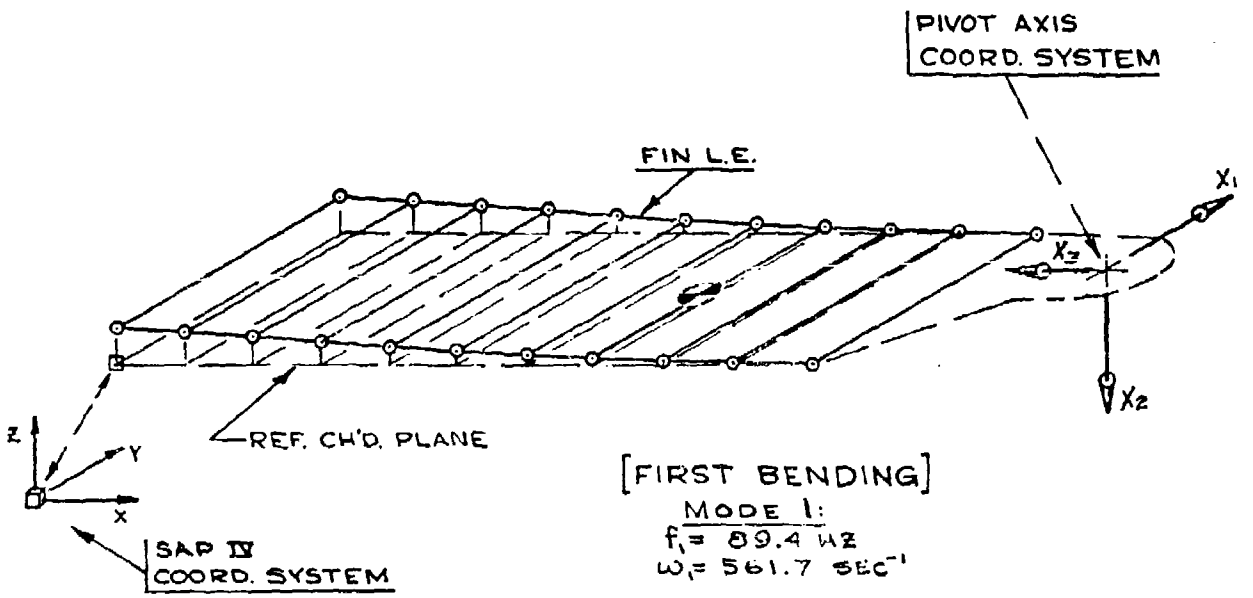

FIG. 6: FIN FIRST BENDING MODE

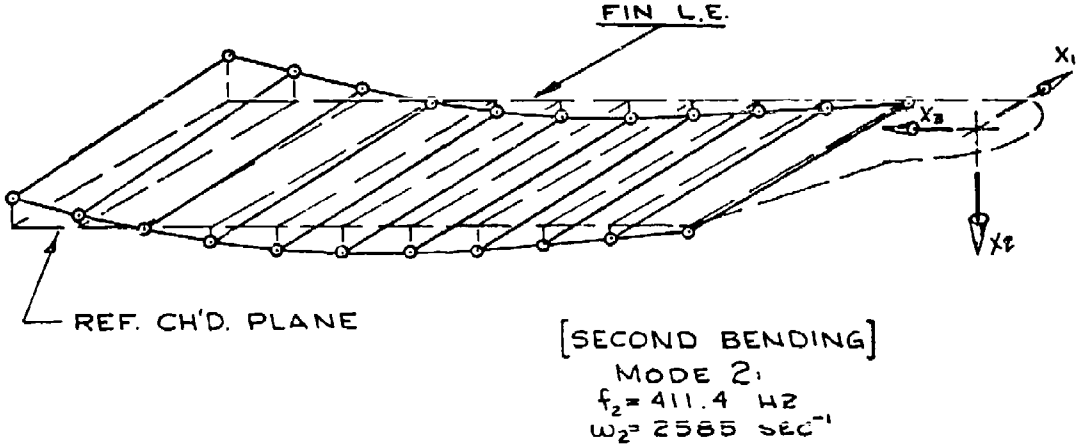

FIG. 7: FIN SECOND BENDING MODE

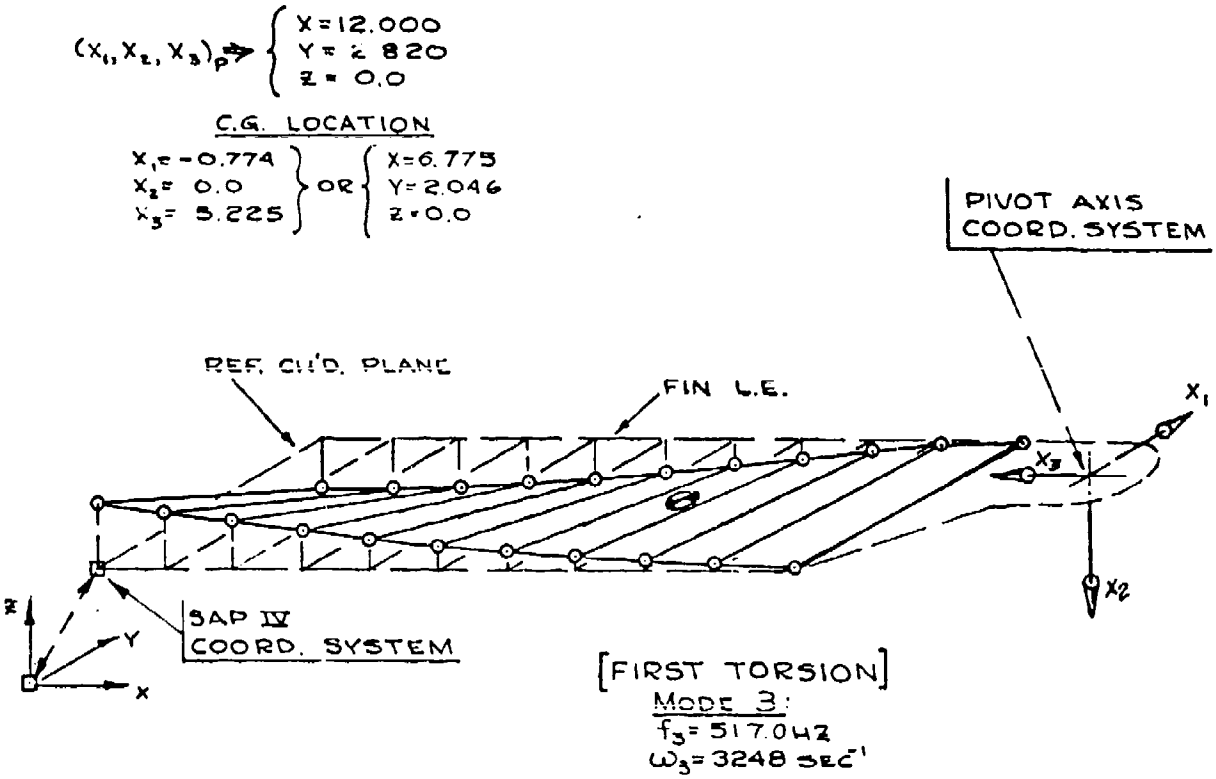

FIG. 8: FIN FIRST TORSION MODE

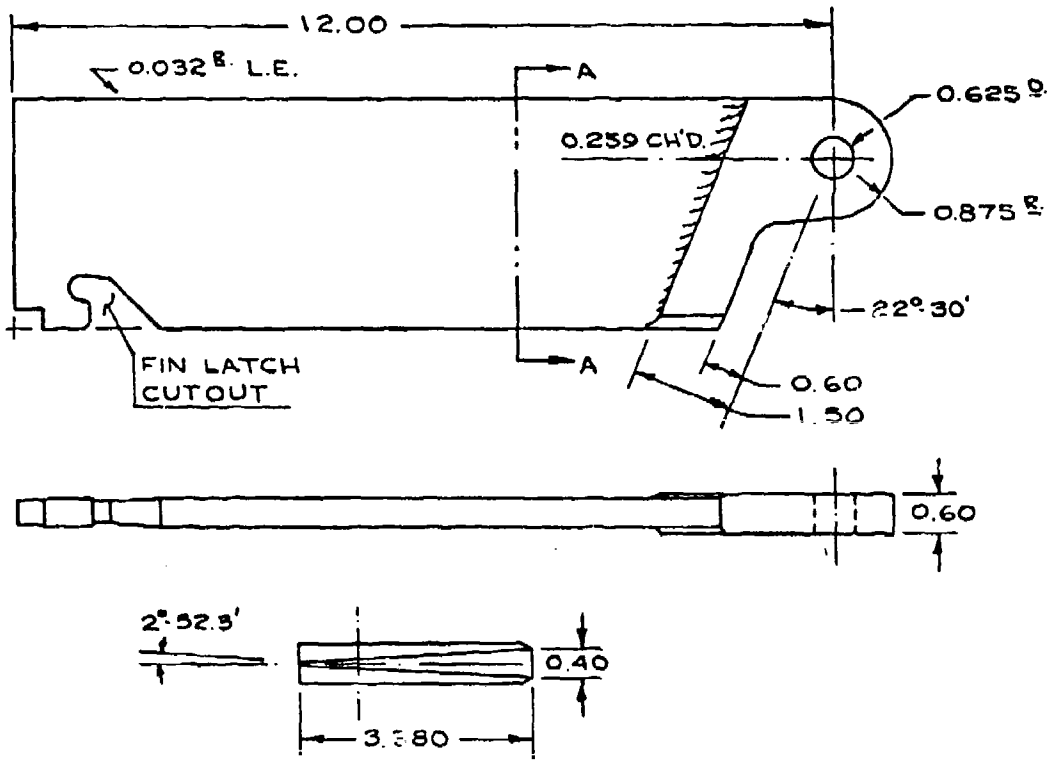

REF.: NWC DWG. SK 450332

FIG. 9: WEDGE FIN GEOMETRY

III. DISCUSSION

A. Background:

The fin-opening dynamics for the gun-launched guided projectile (ERGP) occurs after the spinning ERGP leaves the gun barrel. Upon departing the barrel, a slight initial deceleration of the vehicle causes the release of a fin latch or lock unit, which in turn releases the fins and permits them to open to the fully deployed position under the impetus of the centrifugal accelerations. During the deployment process, angular momentum may be considered as being conserved since other dissipative actions such as aerodynamic roll damping are not of major significance during the initial fin-opening time interval. The fins open until reaching a 60 degree position, when they encounter small cylindrical stops. The fins crush the stops by plastic deformation and then blow back into a detent position corresponding to a 60 degree position, or in an aerodynamic sense, a 30 degree sweepback angle.

Details of the fin-opening process have been obscured because of inherent measurement difficulties in the adverse experimental environment associated with launching from a Naval rifle. Photographic observation of the launch process combined with inspections of the ERGP after recovery has provided clues, which will be used in the ensuing analysis. One significant observation from flight tests has been that the initial roll rate of the ERGP upon departing the rifle was dependent upon the configuration used in the obturator rings. The obturator rings become engraved into the rifling of the gun barrel during launch. The relative slippage between the rings and the ERGP, which is controllable to a limited extent, acts to protect the ERGP from experiencing excessive initial roll rates at launch. However, initial roll rates have been observed up to 30 revolutions per second. Based upon these observations, initial missile roll rates up to 30 RPS will be considered during the parametric variations of the analyses.

B. Crushable Fin Stop:

The rigid fin analysis was used for estimating the magnitude of the moments induced about the fin pivot due to the crushing action of the stops during fin deployment. A sketch of the fin stop is shown on Fig. 10. In estimating the magnitude of the moment required to cause the fin stop to become crushed into a "washer-shaped" object, an assumption of a 120,000 psi ultimate compressive stress led to an

initial guess of 67,800 in-lb total moment reaction at the fin pivot axis for the six fins. This initial value of the crushing-moment level provided by the fin stop was used in a parametric study.

Figure 11 summarizes the effects of the total moment magnitude (from six fins) provided by the crushable stops on the maximum value of opening angle. The assumption was made that fin opening began with an initial missile roll rate of 10 revolutions per second and zero initial fin opening angle rate. Furthermore, on the assumption that initial contact with the fin stop occurred at a fin opening angle of 60 degrees, the fin could be brought to a rest condition by an additional 6 degrees of opening angle if the crushing moment were 40,000 in-lb. Several things to note in the analysis include:

- The original guess of 67,800 in-lbs stopping moment was a startup value for a parametric stuiy only.
- Changes in initial condition of missile roll rate and fin opening angle rate would require different values of crushing moment if the constraint of bringing the fin to a rest condition in 5 to 10 degrees more opening angle after the fin contacted the stop were a valid all encompassing boundary condition.
- The purpose of the crushable stop logic described in section II was solely to provide a mechanism for bringing the fin opening process to a rest condition in a reasonable manner.
- The elastic fin dynamics, in particular the fin's elastic response in bending and torsion, was not critical during the crushing operation.

Since incorporating the logic of the crushable stop for the purpose of arresting the fin opening angle rate was accomplished in a representative manner, and did not lead to any critical bending or torsion responses, further investigation of the fin moment input from crushing the stop did not appear warranted. The actual initial condition range considered in the investigations varied in the following manner:

- $\dot{\Phi}(0)$; t=0 missile roll rate varied from 5 to 30 RPS
- $\dot{\Theta}(0)$; t=0 fin opening rate varied from 0 to 40 rad/sec (2292 deg/sec).

The effects of the above range of initial conditions upon the crushing of the fin stop and consequently the maximum

opening angles are shown on Fig. 12 for the situation of rigid fin dynamics. As will be noted, considering the stopping moment from crushing action as constant (42x10+3 in-lb) did not prevent the maximum opening angle from exceeding 90 degrees when the initial roll rate exceeded 30 RPS. A more refined analysis might have modeled the stopping moment due to plastic crushing of the stop as being a gradual buildup in moment value. The computer logic to implement such a feature is not difficult, but was not employed since the maximum fin elastic deformations in general appeared before the fin stop was contacted during deployment.

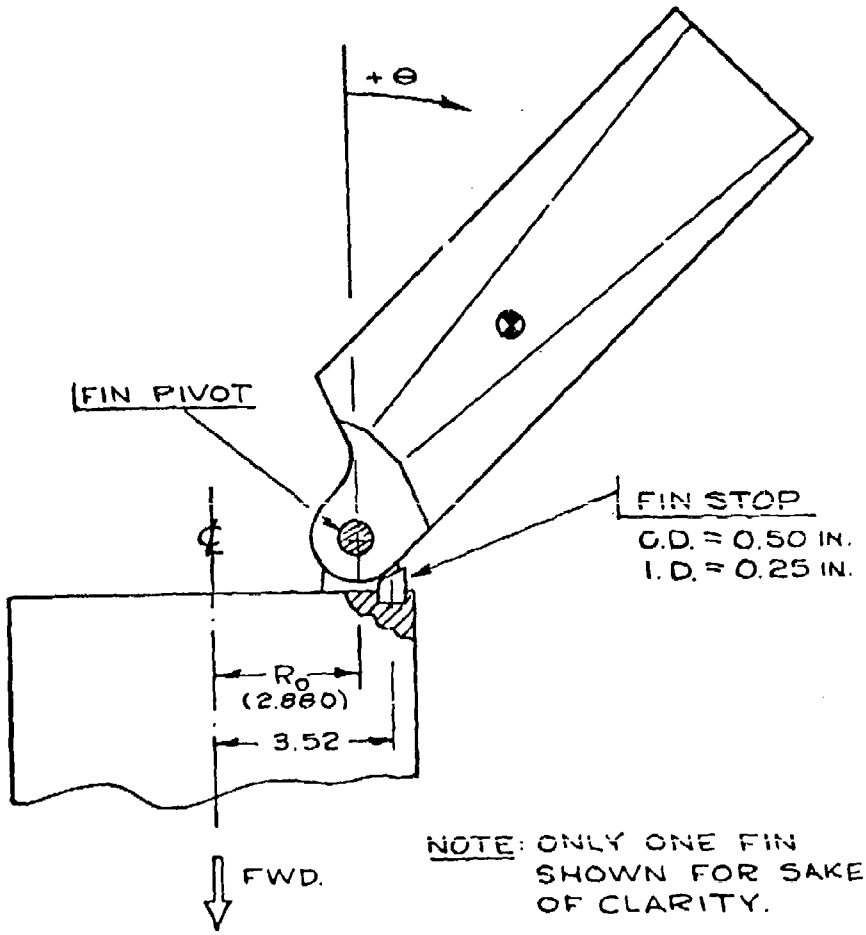

FIG. 10: SKETCH OF FIN STOP

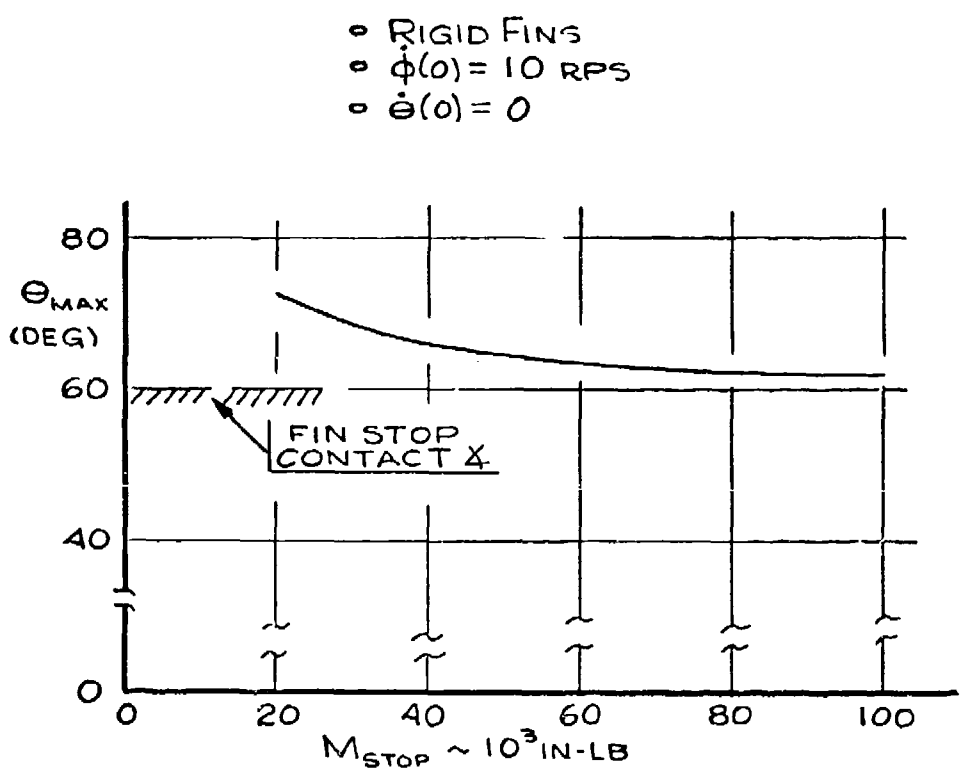

FIG. 11: EFFECTS OF STOPPING MOMENT ON FIN OPENING

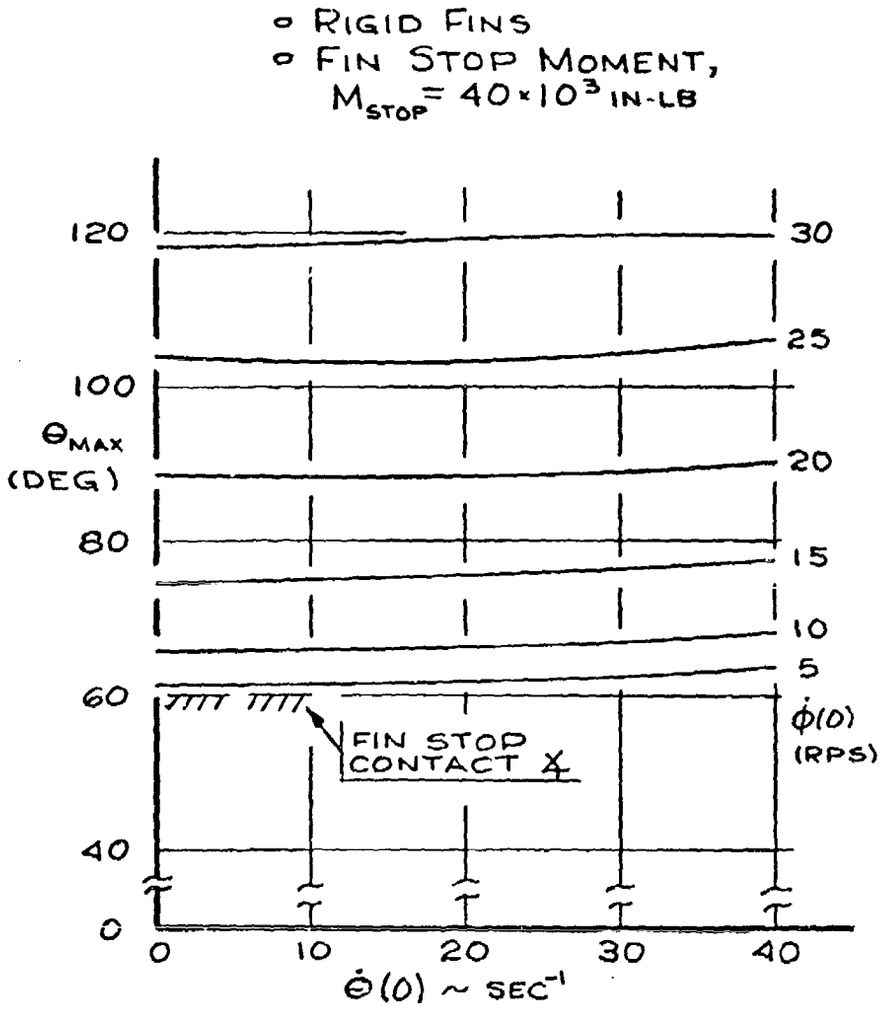

FIG. 12: INITIAL CONDITION EFFECTS ON FIN OPENING

C. Opening Angle Rate:

The time in milliseconds for the fins to reach an opening angle of 60 degrees is shown on Fig. 13 as a function of initial opening rate for various initial values of missile roll rate. Experience from test firings of the ERGP has shown that the condition of the interface between the obturator rings and the missile body allows a reasonable degree of control upon the initial missile roll rate. The opening angle rate, which can be noted on Fig. 13 as having a strong influence upon the fin-opening times, is not as readily amenable to control during testing. Possible factors influencing the intial fin-opening rate would certainly include muzzle gas dynamic interference effects as well as impulsive loadings induced by release of the fin latch.

The latter effect has been estimated in terms of the impulse created by a latch delta-velocity (ΔV) "jump" of one foot per second during latch release. The analysis, details of which may be found in Appendix E, would indicate a sensitivity of 0.66 rad/sec from an one foot/sec velocity "jump" at release for a latch weigning approximately 0.64 pounds.

Unfortunately, it is difficult to estimate the transfer of impulse from the latch into fin-opening rate. However, there is experimental evidence supporting the notion that the fin latch moves forward relative to the ERGP upon the system leaving the gun barrel. The determination of what fraction of the latch's relative forward motion is used as an impulse transfer to initialize the fin-opening rate is a difficult item to quantify since the test environment in the presence of the gun muzzle blast is quite adverse. From an order of magnitude viewpoint, a velocity "jump" from the latch of 50 feet per second for impulse transfer would seem appropriate considering the fact that the latch can encounter an accelerating force due to the gun barrel gas flow (relative to the missile) upon launch.

The inertial properties of the fin were revised to reflect the alternate "wedge" fin shape, Ref. 6, and a rigid fin opening dynamics analysis was performed. The effect of using the wedge fins upon the time to reach a 60 degree opening angle is shown on Fig. 13 by the dashed curves. The wedge fins generally required slightly more time to reach 60 degrees relative to the diamond cross-section fin, Ref. 2, but in general the time difference was on the order of a five percent or less increase.

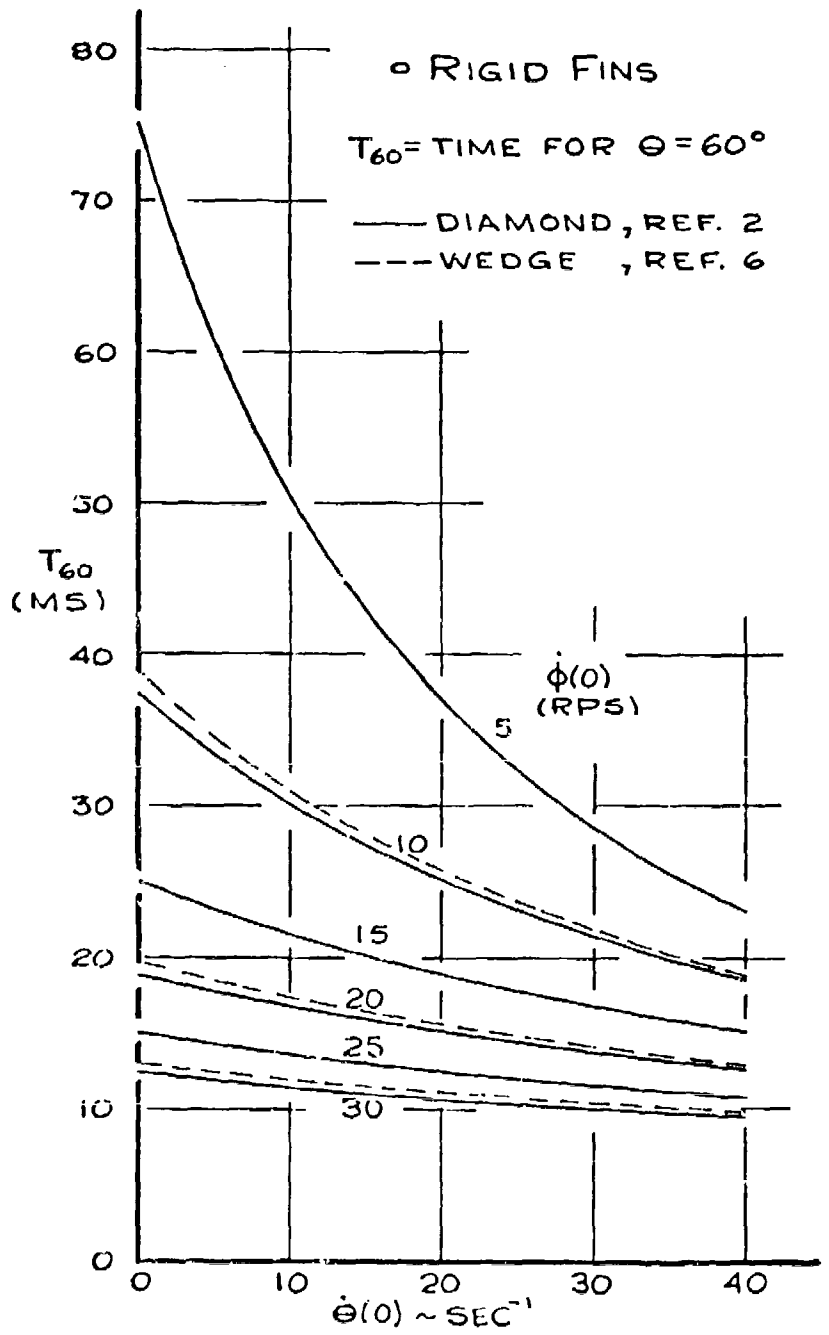

FIG. 13: SUMMARY OF FIN-OPENING TIMES

D. Elastic System Response:

A typical time history plot showing fin opening angle for various opening rate initial conditions at an initial missile roll rate of 10 revolutions per second (RPS) is shown on Fig. 14 for a typical situation of an elastic fin response. The contact by the fin with the crushable stop at 60 degrees opening angle is followed by a short period of deceleration to a zero opening rate condition and is denoted on Fig. 14 by the dashed fairing. Fin elastic effects were not noticable upon the curve shape since angular momentum in the theta (Θ) direction was not directly influenced by fin bending and torsion response. The time to reach 60 degrees of fin opening was increased slightly when fin elasticity was included in the dynamic modeling as a result of fin bending effects having an influence upon missile roll rate time histories, which in turn interacted with fin deployment through a centrifugal force dependence. A first order consideration of opening angle time histories may be viewed as being reasonably well represented by the rigid system model since fin elasticity is not a strong influence upon the theta (Θ) generalized coordinate.

A significant factor in fin deployment is the mass moment of inertia increase about the roll axis. Deploying the fins to the 90 degree position typically increased the 8-inch ERGP roll axis moment of inertia by 25 percent. Angular momentum considerations would lead one to expect a 20 percent decrease (0.80 = 1/1.25) in missile roll rate relative to the initial value at departure from the gun barrel.

The rigid fin roll-rate time history plot is shown on Fig. 15 for an initial roll rate of 10 RPS and varying conditions of initial opening-angle rate. Although the times to reach the 60 degree deployment situation were dependent upon initial conditions, the ratio of deployed system to initial system roll rates remained invariant by the angular momentum conservation considerations stated above. It should be noted that these remarks are applicable only to the system with the rigid fin assumption.

Figure 16 covers the same range of initial conditions as in the preceding figure, except that the dynamic terms from the fin motion included an elastic modeling influence from first bending and torsion modes respectively. The time history curves have the time-to-reach 60 degrees flagged out, and comparison between Figs. 15 and 16 will substantiate the earlier comment that fin elasticity effects were not a dominant influence upon fin opening. But Fig. 16 does show that the inclusion of fin elasticity significantly altered the roll rate time history, and in particular, the

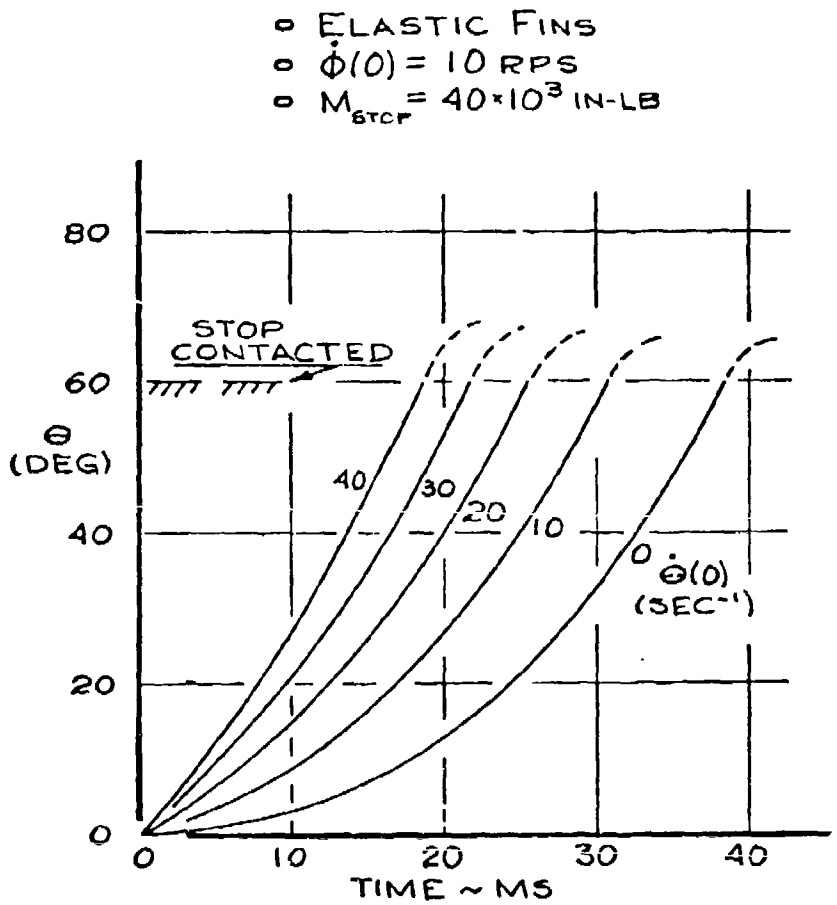

FIG. 14: FIN DEPLOYMENT TIME HISTORIES

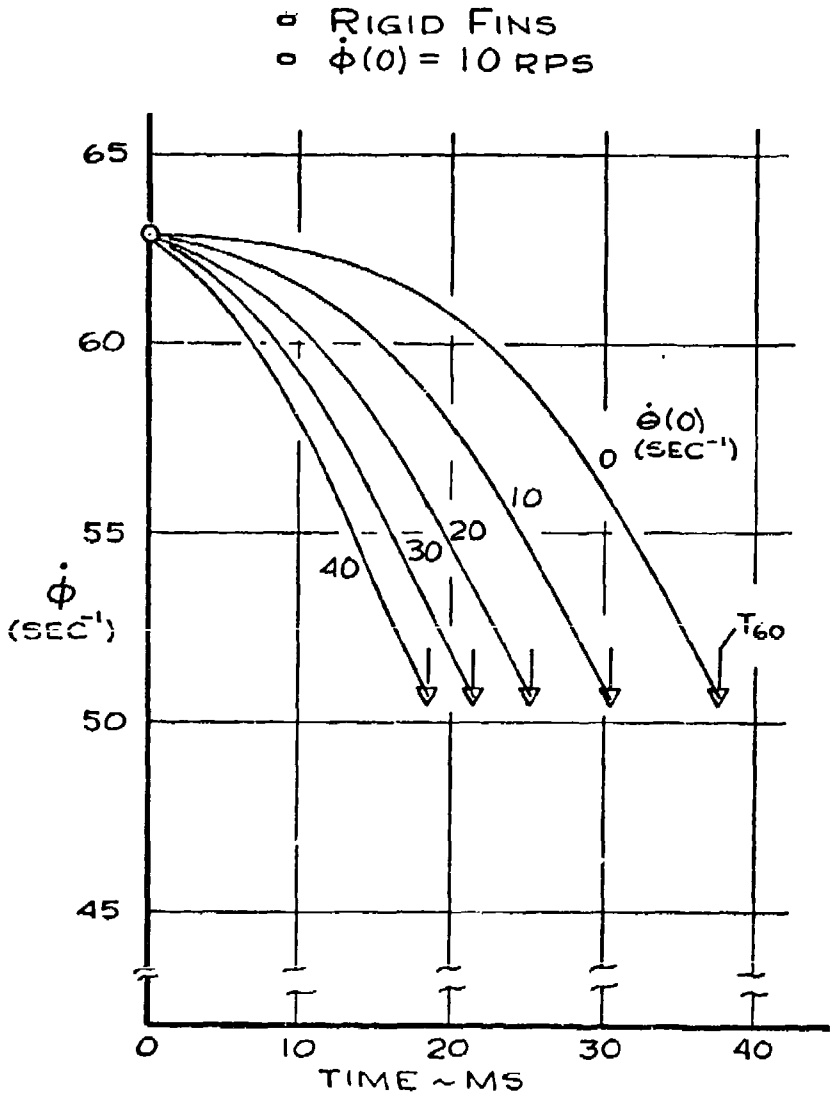

FIG. 15: RIGID FIN ROLL RATE TIME HISTORIES

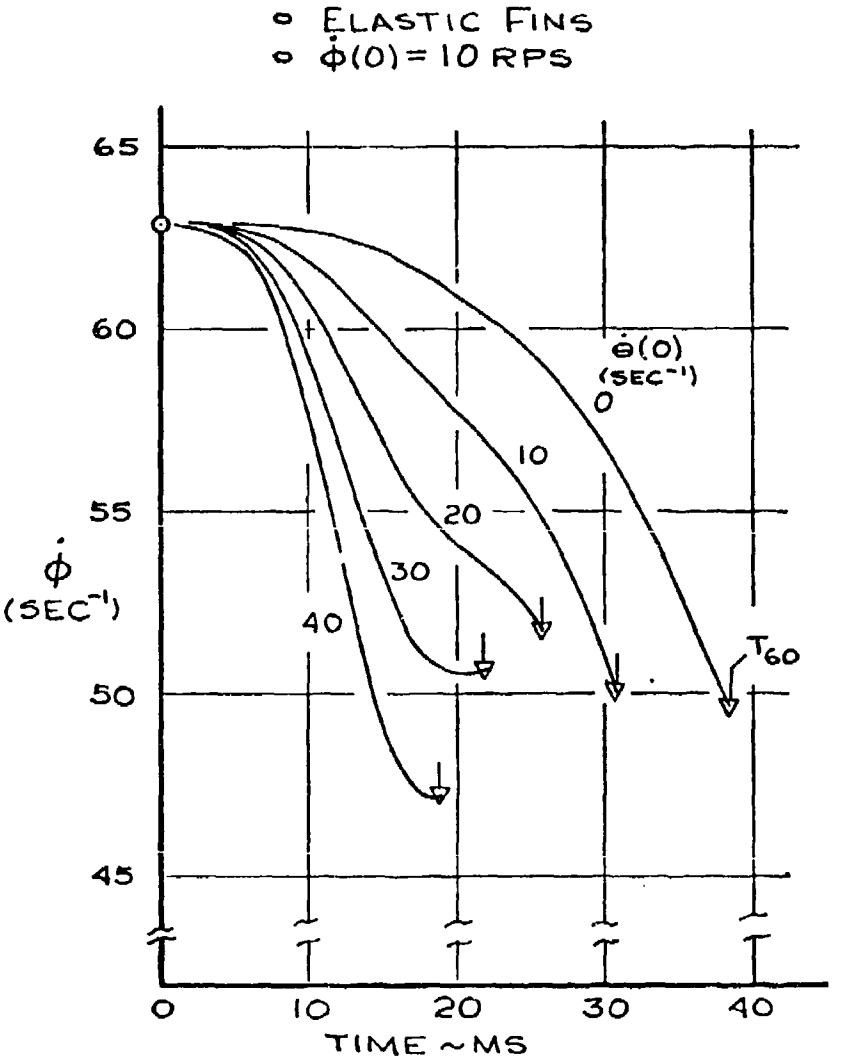

FIG. 16: ELASTIC FIN ROLL RATE TIME HISTORIES

value of missile roll rate when the fins were deployed to 60 degrees was not invariant with fin-opening rate as was the case for the rigid-fin dynamic model. The influence of fin elasticity may be attributed to a coupling between the fin's bending mode and the missile's roll mode. Fin bending motion can be visualized as interacting with angular momentum about the roll axis with an added dependence from the fin deployment angle.

These remarks, concerning the influence of fin elasticity upon roll-rate time histories suggest that difficulties might be experienced in estimating fin-opening performance by photographic observations. It would be quite possible to mistake the influence of fin bending excitation as an unknown error (or "noise") in missile roll rate. In addition, actual photographic evidence of missile roll angle (and hence rate) may occasionally be clouded by the gun barrel blast. It might be difficult to correlate an obturator ring configuration with a transient roll-rate value, expecially if the missile roll rate were to change by 20 to 30 percent during the typical 20 to 30 millisecond opening process.

Another interesting consideration is provided by Fig. 17, which shows the dependence of missile initial condition upon roll angle when 60 degree fin deployment angle is first attained. The family of roll angle curves would indicate that as a general rule, the fins reach the deployed position in less than one-third of a revolution. One point to note is that the roll angle for 60 degrees fin deployment was invariant with missile initial roll rate providing that the fin-opening rate was initially zero. However, this latter observation may be somewhat academic since the evidence from test observations during firing tends to support an assumption of a non-zero initial fin-opening rate.

Representative elastic fin bending response time histories for an initial missile roll rate of 10 RPS may be seen on Fig. 18 for various opening rate initial conditions. Of particular note is that the bending response appears as a superposition of a time varying waveform upon a linearly increasing variation with the amplitude of the wave being dependent upon initial opening angle rate. As may be noted, peak values of bending deflection occur on the second wave for the lower values of initial opening rate and on the first wave at the higher values of initial condition. At the larger values of initial opening rate, the time to reach 60 degrees of opening angle was 20 milliseconds or less and hence the response could accommodate only one wave peak before the action of the crushable fin stop entered into the dynamics.

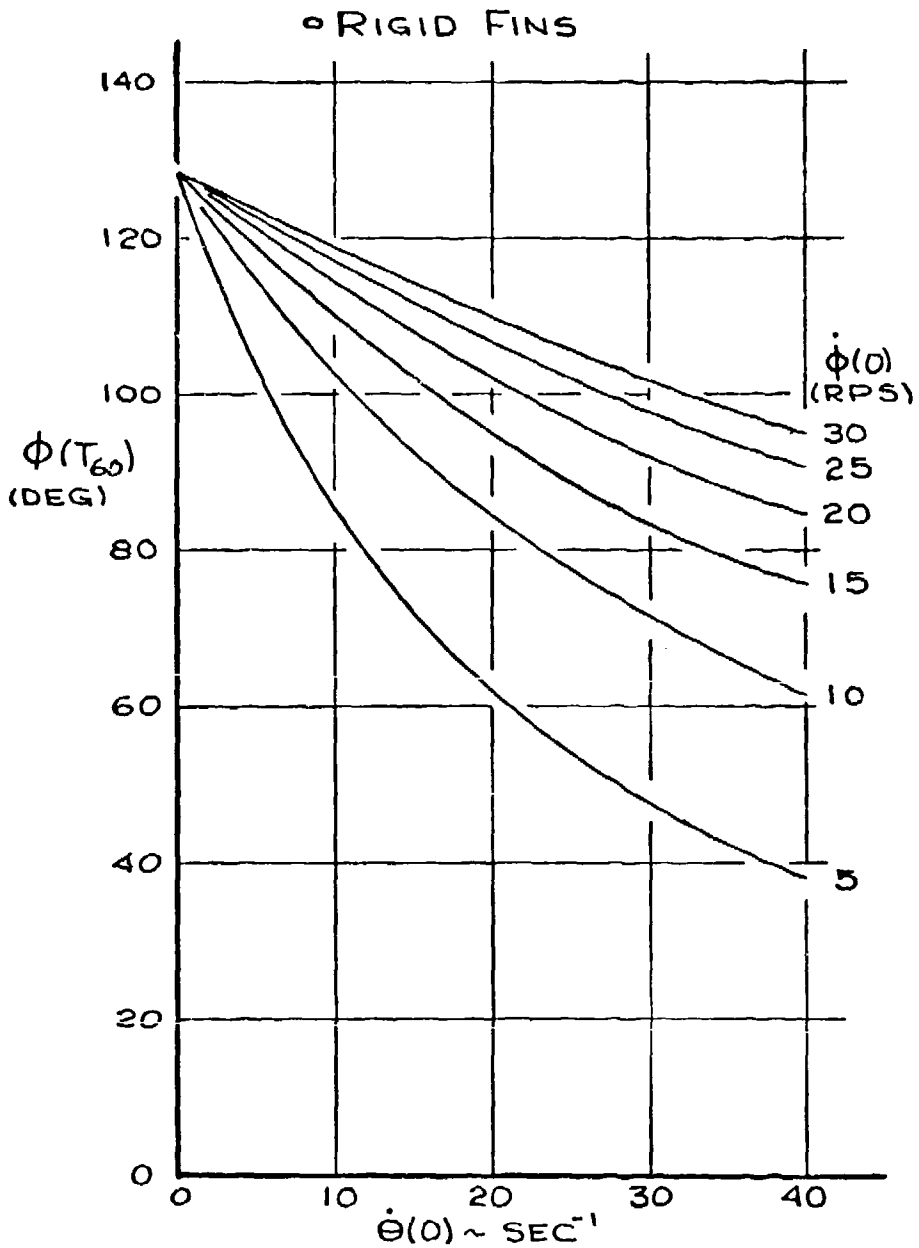

FIG. 17: ROLL ANGLE FOR 60° FIN OPENING

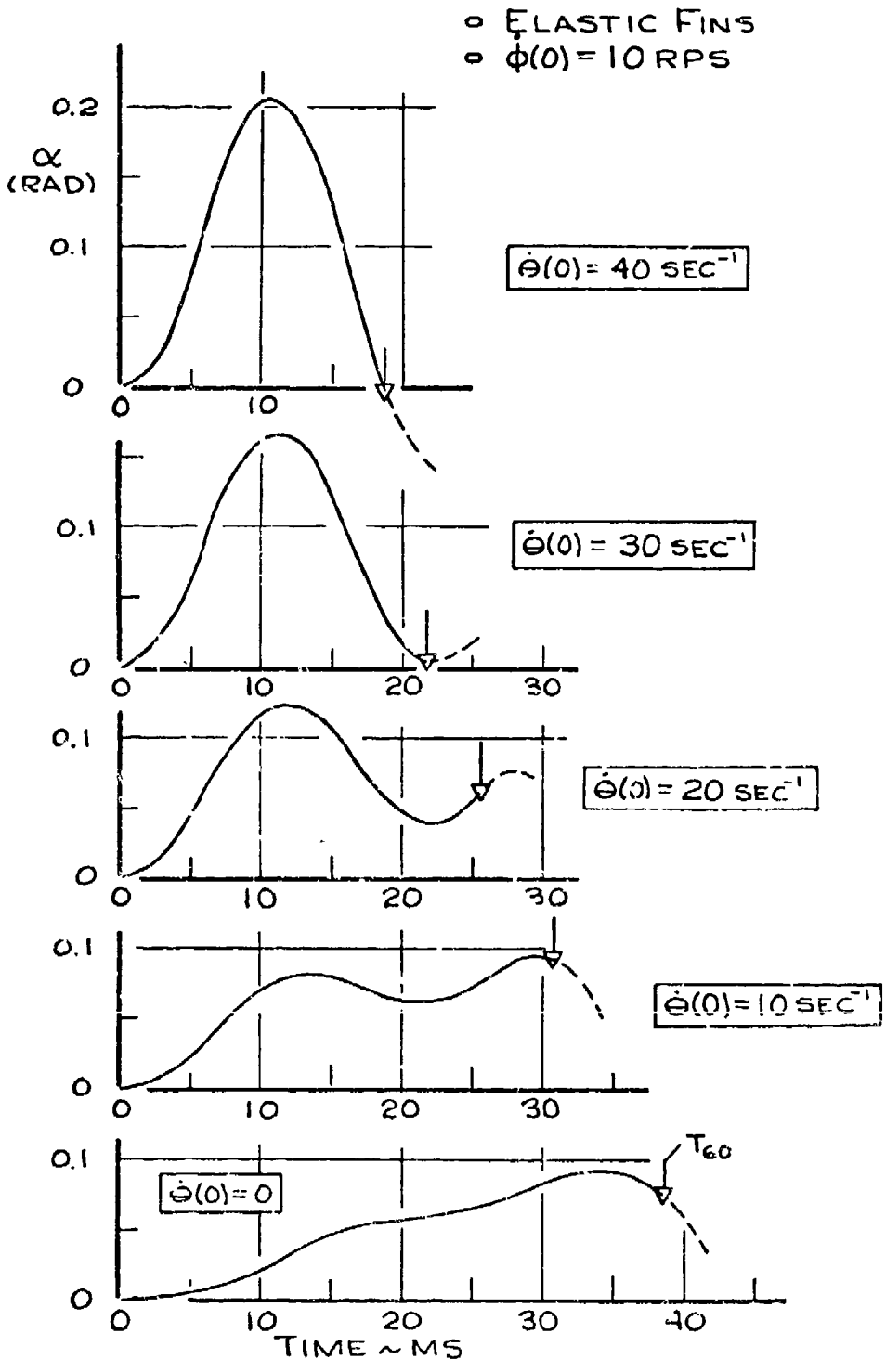

FIG. 18: FIN BENDING TIME HISTORIES

Although the period of the wave was not clear on the curves, Fig. 18, an approximate estimate of 17 milliseconds for a wave period would indicate the presence of a 59 Hz frequency in the transient response. The fundamental frequency of the fin in a non-rotating coordinate system was estimated as 89.4 Hz (c.f., section II-C), which serves to illustrate that the rotating coordinate system does have an influence upon the modal frequencies and consequently, also upon the transient responses. Further investigations of the transient response behavior certainly should consider the effects of higher bending modes as well as a sensitivity study due to changes in the various stiffness constants.

The transient torsional response for the same range of initial conditions as described above may be found on Fig. 19. The curve shapes are similar to those shown for bending response; however, the response magnitude appears reduced by three orders of magnitude. This observation would lead one to consider dynamic modeling of fin elasticity as being primarily dominated by fin bending response.

The main impetus for including fin elasticity in the dynamic model of fin opening was to identify situations when fin root bending stresses could become sufficiently large so as to induce structural yielding. Figure 20 summarizes the peak values of the generalized first bending coordinate for the complete range of initial conditions. An alternate scale is also presented of maximum induced bending stress encountered at the fin root. The corresponding maximum stress scale was based upon translating bending deflection to bending moment using the effective spring stiffness constant, K_α, described in section II-C. If yielding were assumed to occur in the neighborhood of 160,000 psi tensile stress, then evidence of permanent set in the fin bending coordinate could be expected if the initial missile roll rate exceeded 15 to 20 RPS. It should also be noted that the maximum stress encounter was influenced more strongly by initial roll rate rather than by initial fin-opening rate. In order to emphasize the latter comment, Fig. 21 has been prepared to illustrate the peak fin-bending induced stress encounter as a function of initial missile roll rate for several cases of initial fin-opening rate.

Figures 20 and 21 illustrate that the most effective way of avoiding missile residual roll rate due to permanent set of the fins is to configure the obturator rings so that initial missile roll rates are kept below approximately 15 RPS.

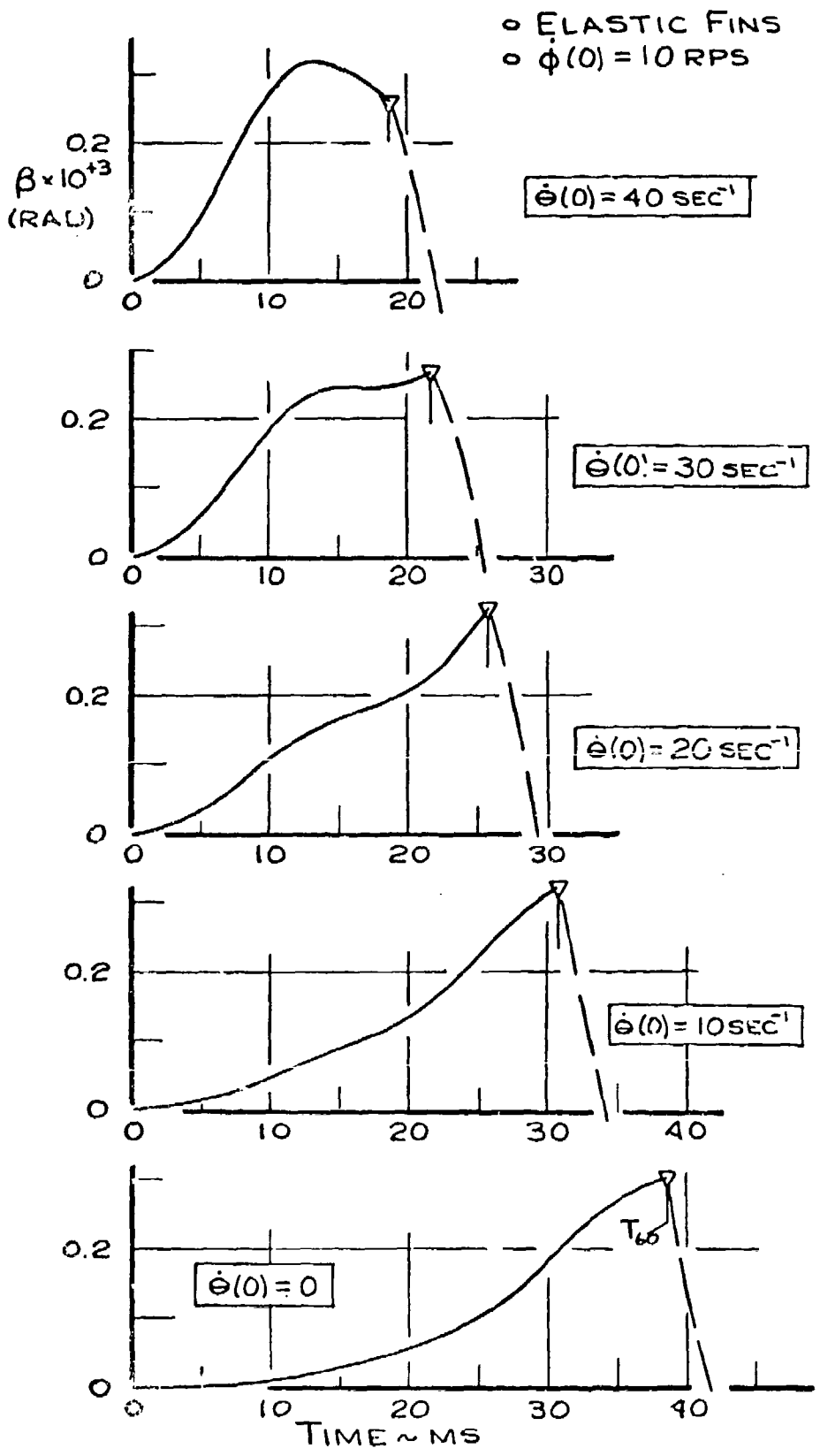

FIG. 19: FIN TORSION TIME HISTORIES

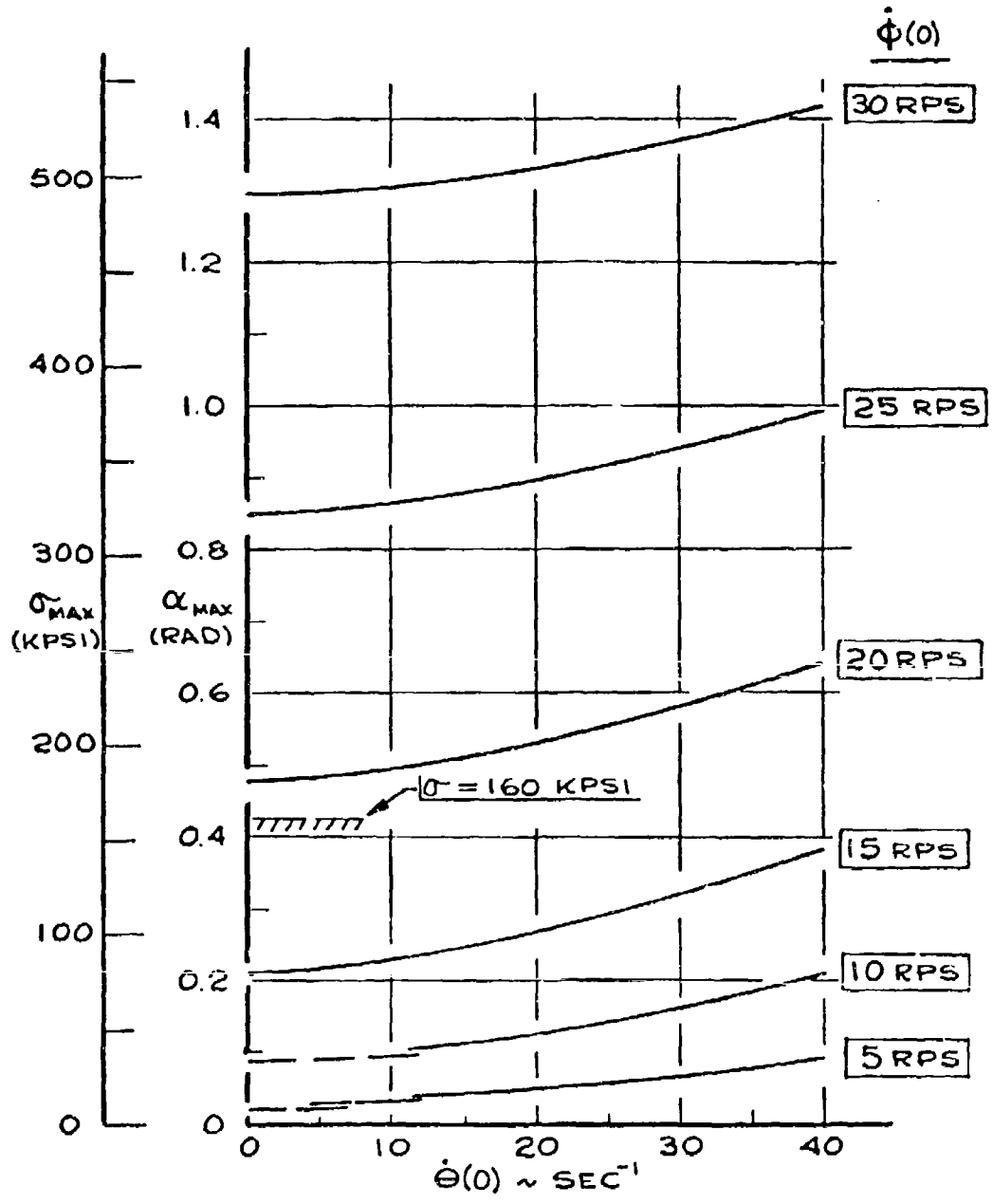

FIG. 20: PEAK FIN BENDING VS. INITIAL OPENING RATE

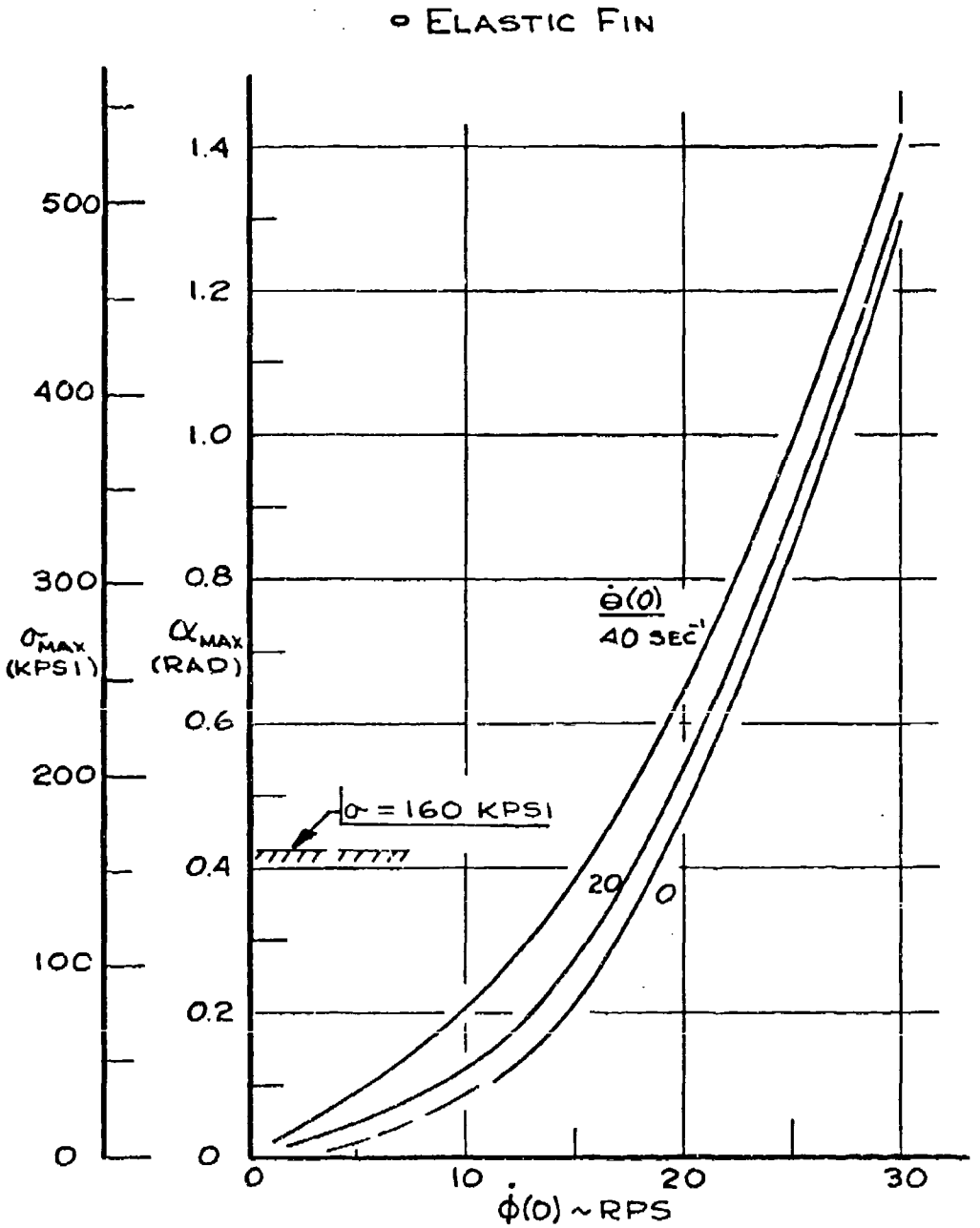

FIG. 21: PEAK FIN BENDING VS. INITIAL ROLL RATE

As an aside, it should be recognized that the linear stress-strain relationship of the fin material, which was an inherent feature of the fin elasticity model, would not be a valid assumption for higher values of initial conditions where material yielding might be expected. However, the curves of peak-stress encounter represent events, which for stresses beyond yielding, only occur for a few milliseconds. Therefore, improvements in the dynamic modeling should also reflect material property dynamics if one were seeking to quantify estimates of fin yielding. Fortunately, the CSMP technique, Ref. 3, allows the convenient inclusion of logic statements that can accommodate improved dynamic modeling in case the scope of the investigations were broadened.

E. Experimental Correlation:

As one would expect from earlier comments made in this report, the acquisition of experimental information for describing fin-opening dynamics was potentially limited, both in amount and scope, because of the adverse nature of the launch environment. A limited amount of fin-opening performance has become available based upon photographic records. Results of this technique, described in Ref. 7, showing the time for 60 degree fin deployment are summarized on Fig. 22. It should be noted that these results are relative to the wedge-shaped fins which are slightly different in properties from the diamond-shaped fins. The latter fin configuration was the principal consideration in this report.

The two faired curves on Fig. 22 represent results from fin-opening spin tests conducted under controlled laboratory conditions and from gun-launched test firings using an 8-inch rifle available at the NWC gun range. The spin test results were assumed to represent a zero initial condition situation for fin-opening rate, while the fin-opening rate was an unknown for the actual gun-launched tests. Table II compares predicted results from the dynamic modeling of a (rigid) wedge-shaped fin with the data points on Fig. 22. For the situation of the spin tests, the predicted values of T_{60} were in general slightly lower by a few milliseconds, using the assumption that the initial opening rate was zero.

The actual gun-launched tests provided values of T_{60} that could be used in an indirect manner to obtain estimates of in-situ initial fin-opening rates. By matching the measured and predicted fin-opening times, initial fin-opening rates were deduced in the range of 33 to 50 rads per second; c.f., Table II. These results add support to the intuitive feeling that the opening rate was due to an effective fin latch ΔV "jump" of approximately 50 feet per second, where it is recognized that the term "effective" was used to cover momentum input sources to fin opening from gun blast dynamic influences as well as the kinematics of the fin latch mechanism. In any event, there does appear to be credence provided relative to the range of fin-opening rates considered in the analysis of the report, as well as to the results of the analysis.

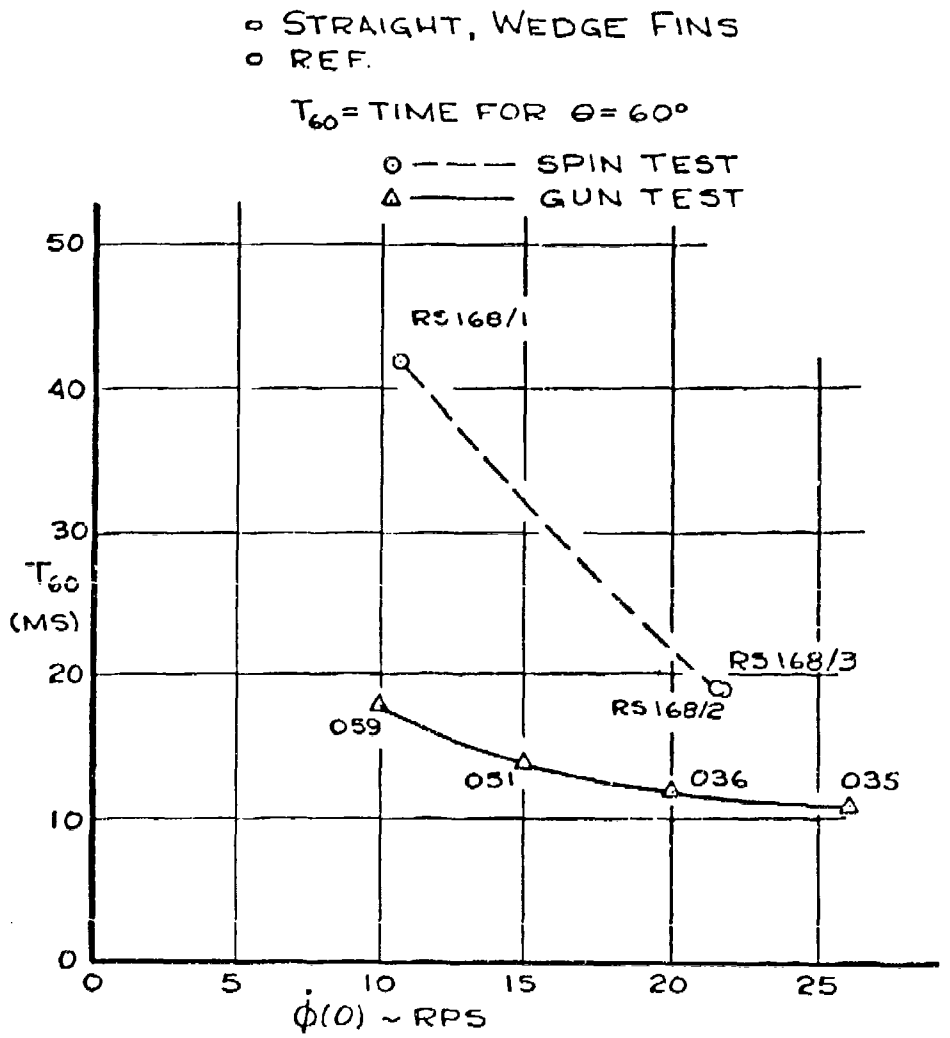

FIG. 22: EXPERIMENTAL FIN-OPENING TIMES

TABLE II

Comparison of Theory and Results
(Beige Fins)

A. Spin Tests:

Ident.	$\dot{\phi}(0)$ RPS	$\dot{\theta}(0)$ sec^{-1}	T_{60} (MS)	
			Meas.	Pred.
RS168/1	11.5	0	42	35.2
RS168/2	23.0	0	19	17.5
RS168/3	23.5	0	19	17.0

B. Gun Tests:

Ident.	$\dot{\phi}(0)$ RPS	T_{60} MS	$\dot{\theta}(0)$ (sec^{-1})	
			Meas.	Pred.
059	10	18.	n.a.	43
051	15	14	n.a.	50
036	20	12	n.a.	48
035	27.2	11	n.a.	33

IV. CONCLUDING REMARKS

An analysis of fin-opening dynamics has been completed for the 8-inch ERGP using four generalized coordinates in conjunction with Lagrange's equations of motion. This method procedurally simplified the derivation for the coupled equations of motion into an algebraic manipulation. The elastic model for representing fin dynamics included both fin bending and torsion response representations. Analyses disclosed that the bending responses dominated the elasticity influences by several orders of magnitude, which result was in accord with independent analyses conducted by Boone, Ref. 7, on a 5-inch gun-launched projectile with a similar fin configuration.

The question of result credibility was addressed by making a comparison with limited experimental results giving opening times, and from these comparisons an added benefit was obtained; namely, an indication that the initial fin-opening rate was in the neighborhood of 35 to 50 radians per second.

Since the results of the report appear physically consistent, one may conclude that the analysis method does provide the systems designer with a tool to describe fin-opening dynamics, including other configurations, in a straightforward manner. Hindsight obtained from the results would suggest that improvements in the elastic model could be made by adding more fin bending degrees of freedom and by incorporating improved logic to accommodate the effects of material yielding.

The residual roll rate for the 8-inch ERGP following the completion of the gun launch, fin-opening transients and roll rate decay by aerodynamic damping is governed by both the initial fin alignment and permanent set induced by structural yielding due to launch and opening dynamics. The latter effects, described as a main goal of these investigations, appeared to be dependent primarily upon the initial missile roll rate and secondarily upon the initial condition of fin-opening angle rate; c.f., Fig. 21. It would appear that most of the problems associated with inertially induced structural yielding by the fins could be avoided if the obturator ring configuration between the missile and the gun barrel were defined for initial missile roll rates below 15 RPS. This philosophy does not eliminate the influence of gun barrel gas dynamics and fin latch momentum transfer into the fin's initial opening rate, but rather it relegates those problems into a subordinate role, which certainly is to be desired when trying to achieve engineering design success.

APPENDIX A

Equations of Motion:

The Lagrange equation approach will be used for setting up the governing relationships for the fin-dynamics problem. The equations will include terms to provide an elementary treatment of the elastic fin response; however, it will become evident in the analysis as to which terms need to be removed for reversion to a rigid-fin situation. The first step in the procedure is to locate the center-of-gravity (c.g.) positions of the various fin elements relative to an inertially oriented reference frame. The next step relates to the development of the system kinetic energy terms, composed of translational and rotational components relative to the individual c.g. locations. The third step involves the establishment of potential energy type terms. Finally, the equations of motion become identified by direct substitution of the appropriate derivative terms in Lagrange's equation.

The contribution to energy from the rotating missile body (without fins) is given by:

$$\Delta T = \tfrac{1}{2} I \dot{\phi}^2$$

and

$$\Delta V = \emptyset \qquad \ldots(A.1)$$

In treating the fin translational contribution to energy, assumptions made will include:

- Fin is modeled by a rigid base plus an elastic fin blade section. The fin base is pin connected to the missile body at a distance R_o from the missile axis of symmetry.
- Fin elasticity considers only the fundamental bending and torsion modes using a simple pendulum model.
- Fin base dynamics can be obtained from rigid-fin modeling by appropriate revisions to the c.g. and mass terms.

--- Fin Base Kinetic Energy ---

The absolute position of the fin base c.g. relative to the inertial coordinate frame of reference, x_1', x_2' and x_3' (Fig. 1) for the base may be expressed as:

$$x_{1B}' = \left[R_o + X_{1B}\cos\Theta + X_{3B}\sin\Theta\right]\cos\phi$$

$$x_{2B}' = \left[R_o + X_{1B}\cos\Theta + X_{3B}\sin\Theta\right]\sin\phi \qquad \ldots(A.2)$$

$$x_{3B}' = -X_{1B}\sin\Theta + X_{3B}\cos\Theta$$

where numerical values for R_o, x_{1B} and x_{3B} may be found in Table I. The next step is to take the time derivative of the inertial position, followed by summing the squares to obtain the square of the velocity; i.e.,

$$v_B^2 = (\dot{x}'_{1B})^2 + (\dot{x}'_{2B})^2 + (\dot{x}'_{3B})^2 \qquad \ldots(A.3)$$

The translational contribution to kinetic energy for six (6) fin bases, following algebraic simplification, becomes:

$$\Delta T_{B_{TR}} = \tfrac{6}{2} M_B V_B^2$$

$$= 3 M_B \left\{ \dot{\phi}^2 \left[R_o^2 + x_{1B}^2 \cos^2\theta + x_{3B}^2 \sin^2\theta + 2 R_o (x_{1B} \cos\theta + x_{3B} \sin\theta) + x_{1B} x_{3B} \sin 2\theta \right] + \dot{\theta}^2 \left[x_{1B}^2 + x_{3B}^2 \right] \right\} \qquad \ldots(A.4)$$

The rotational contribution to kinetic energy requires expressing the angular velocities of the fin's x_1, x_2 and x_3 coordinate system (ω_1, ω_2 and ω_3 respectively) in terms of an inertial frame of reference. Two coordinate rotations are involved to describe the rigid fin angular rotation consisting of first, a rotation ϕ about the missile axis of symmetry followed by a rotation θ about the fin pivot axis. It should be recognized that this is considerably simpler than the Euler angle approach which is the classical treatment applied in the more general situation when developing angular momentum conservation relations for a rigid body, be it either a gyroscope or an airplane.
Consequently one obtains that:

$$\omega_1 = -\dot{\phi} \sin\theta$$
$$\omega_2 = \dot{\theta} \qquad \ldots(A.5)$$
$$\omega_3 = \dot{\phi} \cos\theta$$

which provides the entries for the rotational contributions to kinetic energy (for 6 fins) as follows:

$$\Delta T_{B_{ROT}} = 3 \left[I_{1B} (-\dot{\phi} \sin\theta)^2 + I_{2B} \dot{\theta}^2 + I_{3B} (\dot{\phi} \cos\theta)^2 \right] \qquad \ldots(A.6)$$

--- Fin Base Potential Energy ---

The contribution of the fin base model to system potential energy would depend upon the relative importance of terms such as the earth's gravitational field or fin elastic deformations. The former was considered as a negligible factor for the rotating missile environment while the latter effect was precluded by the lack of identifiable springs in

the base area. One should note that there is a crushable stop present in the system which absorbs energy after the fin opening angle, Θ, has reached 60 degrees. The logic required for this effect will be treated separately later. Therefore, based upon these arguments, we shall assume that:

$$\Delta V_B = 0 \qquad \ldots(A.7)$$

--- Fin Blade Kinetic Energy ---

In modeling fin elasticity according to the stated assumptions, the fin was considered to deflect in bending deformation as an equivalent pendulum with angle α about a virtual pivot located on the chord plane at the top of the fin base. Symmetry conditions were assumed for the elastic fin about the midchord line. Hence, the absolute position of the elastic fin c.g. relative to the inertial coordinate frame of reference, x_1', x_2' and x_3' (Fig. 1) may be expressed in a form similar to eqn. A.2 as:

$$\begin{aligned} x'_{1F} &= \left[R_o + X_{1F}\cos\Theta + X_{3F}\sin\Theta\right]\cos\phi + \Delta X_3 \sin\phi\,\alpha \\ x'_{2F} &= \left[R_o + X_{1F}\cos\Theta + X_{3F}\sin\Theta\right]\sin\phi - \Delta X_3 \cos\phi\,\alpha \\ x'_{3F} &= -X_{1F}\sin\Theta + X_{3F}\cos\Theta \end{aligned} \qquad \ldots(A.8)$$

The numerical values involved in the above relations are stated in Table I. The term Δx_3 is the distance in the x_3 direction (spanwise for the fin) from the virtual pivot of the simple pendulum model to the elastic fin c.g.. The above equations include a small angle assumption upon the bending angle deformation; i.e., $\alpha \cong \sin\alpha$.

The translation contribution of the six (6) elastic fins to kinetic energy may be evaluated in a manner similar to the development that led to eqn. A.4. Results were:

$$\begin{aligned} \Delta T_{F_{TR}} = 3 M_F \Big\{ & \dot\phi^2 \left[R_o^2 + X_{1F}^2\cos^2\Theta + X_{3F}^2\sin^2\Theta + \right. \\ & \left. + 2R_o(X_{1F}\cos\Theta + X_{3F}\sin\Theta) + X_{1F}X_{3F}\sin 2\Theta + \Delta X_3^2\alpha^2\right] \\ & + \dot\Theta^2\left[X_{1F}^2 + X_{3F}^2\right] + \Delta X_3^2\,\dot\alpha^2 \\ & + 2\dot\phi\dot\Theta\left[-X_{1F}\sin\Theta + X_{3F}\cos\Theta\right](\Delta X_3\,\alpha) \\ & - 2\dot\phi\dot\alpha\left[R_o + X_{1F}\cos\Theta + X_{3F}\sin\Theta\right](\Delta X_3)\Big\} \end{aligned} \qquad \ldots(A.9)$$

For the elastic fin model, the angular velocity components of eqn. A.5 become modified by inserting bending and torsion angle deflection rates, as noted below:

$$\omega_1 = -\dot{\phi}\,\text{SIN}\,\theta + \dot{\alpha}$$

$$\omega_2 = \dot{\theta} \qquad \ldots(A.10)$$

$$\omega_3 = \dot{\phi}\cos\theta + \dot{\beta}$$

The contribution of rotation to kinetic energy for the six elastic fins is obtained by applying eqn. A.10, which yields:

$$\Delta T_{F_{ROT}} = 3\left\{ I_{1F}(-\dot{\phi}\,\text{SIN}\,\theta + \dot{\alpha})^2 + I_{2F}\,\dot{\theta}^2 + I_{3F}(\dot{\phi}\cos\theta + \dot{\beta})^2 \right\} \qquad \ldots(A.11)$$

--- Fin Blade Potential Energy ---

The elastic modeling of the fin as a simple pendulum in both bending and torsion allows us to express the potential energy for the six fins as:

$$\Delta V_F = 3\left[K_\alpha \alpha^2 + K_\beta \beta^2 \right] \qquad \ldots(A.12)$$

In the above expressions, the estimate for the elastic spring constants were obtained from the separate free vibration calculations of the finite element fin model using the structural analysis program known as SAP IV.

--- Crushable Stop Energy Model ---

The last item for inclusion in the energy formulation is the crushable stop which is used to bring the fin to a rest condition during the opening process. The crushable stop, one per blade, is a small steel cylinder positioned on the missile base frame in a manner such that the fin base makes initial contact at a fin opening angle, θ, of approximately 60 degrees (1.047 radians). The fin contact with the stop is initially an elastic deformation over a small change in opening angle, but once material yielding has occurred, the influence would correspond to plastic deformation. Therefore, the work from the absorption term will be modeled as an equivalent potential energy term by an expression for the six fins as stated below:

$$\Delta V_S = \begin{cases} 0 & \text{for} \quad \theta \text{ .LT. } 1.047 \text{ rad} \\ 6\,K_S(\theta - 1.047) & \text{for} \quad \theta \text{ .GE. } 1.047 \text{ rad} \\ & \text{and } d\theta/dt \text{ .GT. } 0 \end{cases} \qquad \ldots(A.13)$$

where K_S is an estimate of the stopping moment developed by the plastic type deformation of the crushed stop during the deceleration of the fin opening angle. The actual digital computation will cease (by a logic test) when the angular

rate of opening angle reaches zero. In practice, the fins will then blow back due to the aerodynamic type moments into the detent (locked) position of 60 degrees.

--- Summary of Energy Terms ---

The virtues of a systematic energy formulation for a complex system will now become evident since the establishment of the appropriate coefficients in the equations of motion becomes simplified to a routine algebraic accounting procedure. First, the kinetic energy terms may be summarized in their entirety as:

$$T = \Delta T + \Delta T_{B_{TR}} + \Delta T_{B_{ROT}} + \Delta T_{F_{TR}} + \Delta T_{F_{ROT}} \quad \ldots(A.14)$$

where the contributions to the right hand side are defined by eqns. A.1, A.4, A.6, A.9 and A.11 respectively.

Next, the potential energy terms in their entirety are:

$$V = \cancel{\Delta V^{\phi}} + \cancel{\Delta V_B^{\phi}} + \Delta V_F + \Delta V_G \quad \ldots(A.15)$$

where the contributions to the right hand side have been established by eqns. A.1, A.7, A.12 and A.13 respectively.

--- Definition of Coefficients ---

Equation 3, which is Lagrange's equation for establishing the differential equations that describe the fin-opening dynamics, is restated below for sake of clarity:

$$\frac{d}{dt}\left(\frac{\partial T}{\partial \dot{q}_i}\right) - \frac{\partial T}{\partial q_i} + \frac{\partial V}{\partial q_i} = 0 \quad (i = 1, 2, 3 \text{ and } 4) \quad \ldots(3)$$

where

$$q_1 = \Phi \ , \ q_2 = \Theta$$

$$q_3 = \alpha \ , \ q_4 = \beta$$

The above set of four coupled differential equations may be expanded term by term using the kinetic and potential energy expressions of eqns. A.14 and A.15. In the expansion of the first energy term of eqn. 3, it is convenient to use a matrix format as follows:

$$\frac{d}{dt}\left(\frac{\partial T}{\partial \dot{q}_i}\right) \Longrightarrow \left[A\right]\left\{\ddot{q}\right\} \quad \ldots(A.16)$$

where the square matrix A will in general be symmetric but non-diagonal in character. Term by term expansions of the kinetic energy expression yielded the following coefficients for the A matrix:

$$A_{11} = \left[I + 6MR_o^2\right] + 6\left\{\left[I_1 + Mx_3^2\right]\sin^2\Theta + \left[I_3 + Mx_1^2\right]\cos^2\Theta + \right.$$
$$+ \left[M_B x_{1B} x_{3B} + M_F x_{1F} x_{3F}\right]\sin 2\Theta +$$
$$\left. + 2MR_o\left[x_1\cos\Theta + x_3\sin\Theta\right] + M_F \Delta x_3^2 \alpha^2 \right\}$$

$$A_{22} = 6\left[I_2 + M(X_1^2 + X_3^2)\right]$$

$$A_{33} = 6\left[I_{1F} + M_F \Delta X_3^2\right]$$

$$A_{44} = 6\, I_{3F}$$

$$A_{12} = A_{21} = 6\, M_F\left[X_{3F}\cos\theta - X_{1F}\sin\theta\right]\Delta X_3\,\alpha$$

$$A_{13} = A_{31} = -6\left\{M_F R_o \Delta X_3 + \left[I_{1F} + M_F X_{3F}\Delta X_3\right]\sin\theta + M_F X_{1F}\Delta X_3\cos\theta\right\}$$

$$A_{14} = A_{41} = 6\, I_{3F}\cos\theta$$

$$A_{23} = A_{32} = 0$$

$$A_{24} = A_{42} = 0$$

$$A_{34} = A_{43} = 0 \qquad \ldots(A.16a)$$

It is convenient to rearrange the equations of motion into matrix form (eqn. 4) as:

$$\left[A\right]\left\{\ddot{q}\right\} = \left\{g\right\} \qquad \ldots(4)$$

where the column vector, g , is derived from:

$$\frac{\partial T}{\partial q_i} - \frac{\partial V}{\partial q_i} \Longrightarrow \left\{g\right\} = \left\{g(q,\, \dot{q},\, t)\right\} \qquad \ldots(A.17)$$

The first component of the g column vector, when expanded, becomes:

$$g_1 = b_{12}\dot{q}_1\dot{q}_2 + b_{13}\dot{q}_1\dot{q}_3 + b_{22}\dot{q}_2^2 + b_{23}\dot{q}_2\dot{q}_3 + b_{24}\dot{q}_2\dot{q}_4$$

where $\ldots(A.17a)$

$$b_{12} = -6\left\{\left[(I_1 - I_3) + M(X_3^2 - X_1^2)\right]\sin 2\theta + 2M R_o\left[X_3\cos\theta - X_1\sin\theta\right] + 2\left[M_B X_{1B} X_{3B} + M_F X_{1F} X_{3F}\right]\cos 2\theta\right\}$$

$$b_{13} = -12\, M_F \Delta X_3^2\,\alpha$$

$$b_{22} = 6\, M_F\left[X_{1F}\cos\theta + X_{3F}\sin\theta\right]\Delta X_3\,\alpha$$

$$b_{23} = 6\, I_{1F}\cos\theta$$

$$b_{24} = 6\, I_{3F}\sin\theta$$

The second component of the g column vector is:

$$g_2 = c_{11}\dot{q}_1^2 + c_{13}\dot{q}_1\dot{q}_3 + c_{14}\dot{q}_1\dot{q}_4 + f_s \qquad \ldots(A.17b)$$

where

$$c_{11} = 3\left[(I_1 - I_3) + M(X_3^2 - X_1^2)\right]\sin 2\theta + 6MR_0\left[X_3\cos\theta - X_1\sin\theta\right] + \\ + 6\left[M_B X_{1B} X_{3B} + M_F X_{1F} X_{3F}\right]\cos 2\theta$$

$$c_{13} = -6\, I_{1F}\cos\theta$$

$$c_{14} = -6\, I_{3F}\sin\theta$$

$$f_5 = \begin{cases} 0 & \text{for } q_2 \text{ .LT. } 1.047 \text{ rad} \\ -6\, K_5 & \text{for } q_2 \text{ .GE. } 1.047 \text{ rad and } dq_2/dt \text{ .GT. } 0 \end{cases}$$

The third component of the g column vector is:

$$g_3 = d_{11}\dot{q}_1^2 + d_{12}\dot{q}_1\dot{q}_2 + f_{33}q_3 \qquad \ldots(A.17c)$$

where

$$d_{11} = 6\, M_F \Delta X_3^2 \alpha$$

$$d_{12} = 6\left\{I_{1F}\cos\theta + 2\, M_F\left[X_{3F}\cos\theta - X_{1F}\sin\theta\right]\Delta X_3\right\}$$

$$f_{33} = -6\, K_\alpha$$

The fourth component of the g column vector is:

$$g_4 = e_{12}\dot{q}_1\dot{q}_2 + f_{44}q_4 \qquad \ldots(A.17d)$$

where

$$e_{12} = 6\, I_{3F}\sin\theta$$

$$f_{44} = -6\, K_\beta$$

A scrutiny of the preceding term by term developments will disclose that the option of rigid-fin dynamics is obtained by dropping terms involving the q_3 and q_4 generalized coordinates and their corresponding coefficients. The "A" matrix reduces to a 2x2 matrix in the rigid-fin situation as an illustrative example.

APPENDIX B

Fin-Dynamics Computer Software:

The computation of fin-opening dynamics as a time history was numerically determined using the Continuous System Modeling Program (CSMP) as documented by Speckhart and Green, Ref. 3. The numerical treatment for solving sets of second order differential equations is similar to the analog computer approach in that the first step is the determination of the highest order derivative(s) followed by succesive integrations. Each integration step allows the introduction of appropriate initial conditions.

The equations of motion have been represented conceptually in matrix form, eqn. 4, for ease of visualization. It will be noted that the equations were inertially coupled as developed by the Lagrange equation formulation technique which is detailed in Appendix A. An analog computer solution approach could accommodate the inertial coupling, but would have difficulties in representing the nonlinear terms. A digital approach can handle the nonlinear terms, but does require that the equations appear as being uncoupled in an inertial sense. The inertial uncoupling, as mentioned in the main section, was achieved by premultiplying the equations of motion by the inverse of the inertial coefficient matrix; i.e., A^{-1} . The existence of the inverse can be argued on the basis of physical considerations. Once the second time derivatives of the generalized coordinates have been determined in an uncoupled form, it is a simple procedure to obtain lower order derivatives by using a fourth order Runge-Kutta integration scheme.

The numerical approach for obtaining fin-opening dynamics by the CSMP method was selected based upon its being user oriented to any person with FORTRAN programming skills. The technique emphasized simplified input data and output result statements respectively. In addition, program control statements were almost a direct description of the mathematical equations or physical variables of the problem. The authors of CSMP contend that the technique allows the user to concentrate on the details of the physical system rather than the usual concerns of numerical analysis and programming. The author of this report is in accord with the contention. It was a pleasant surprise to find that a small investment of time in learning the method produced good dividends in the form of results.

Figure B.1 shows a program flow chart in order to illustrate the procedural simplicity. The CSMP technique identified the solution flow in phases. For the problem at

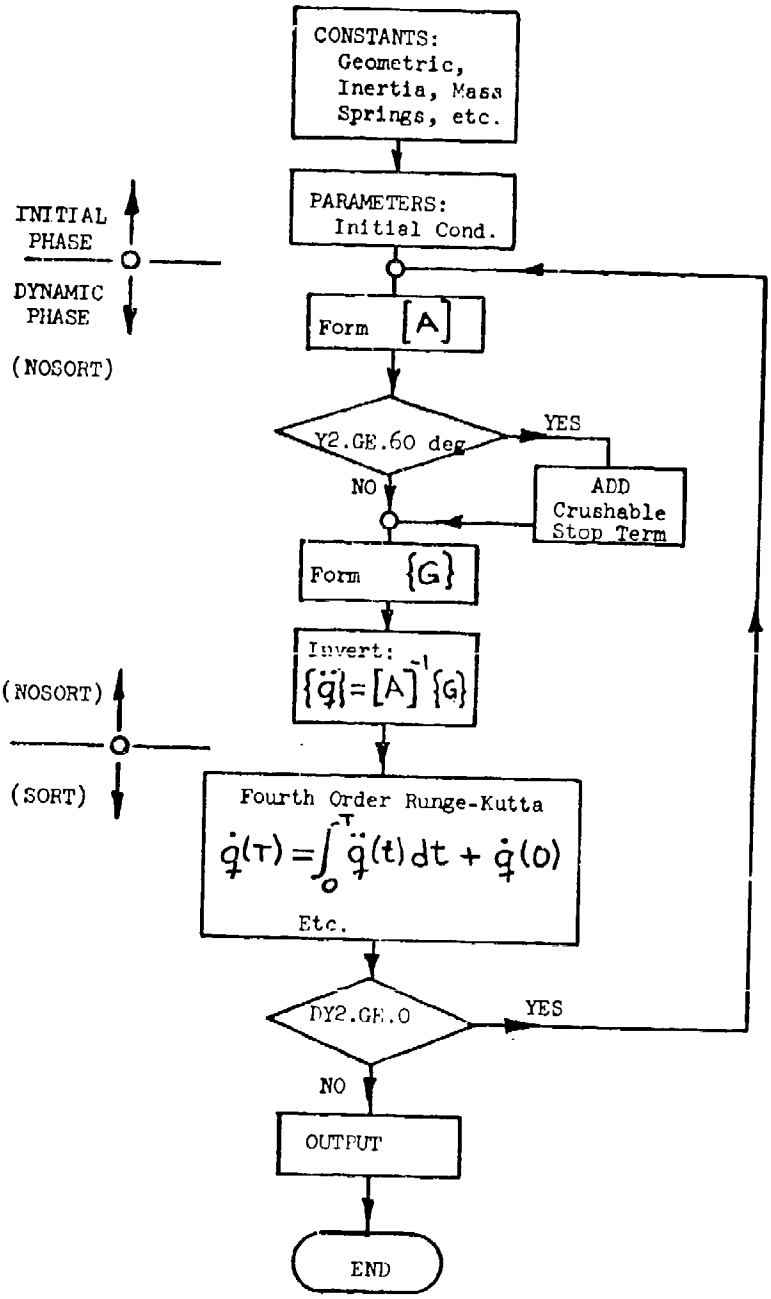

FIG. B-1: PROGRAM FLOW CHART

hand, only the "initial" and "dynamic" phases were required. As one would suspect, the initial phase allowed the entry to the problem of constants and parameters. The initial condition of fin-opening angle rate was normally selected as a problem parameter while the initial missile roll rate was considered as a problem constant. There is a program option to repeat the calculations with changes being made in the constants. This latter option aided considerably to program flexibility, and was used to advantage after the program was debugged.

The dynamic phase is recognizable as the portion of the program that is involved in the computation of the time histories. There are two options available, a "SORT" and a "NOSORT" condition. The "NOSORT" option allows the use of FORTRAN program logic as entered by the programmer with the computational steps being as specified. This section can draw upon subroutines for program support as in more conventional software. For this problem, the "NOSORT" section involved an interaction of all the current variables at any given instant, which is recognized as an inherent trait of a nonlinear problem. The fourth order Runge-Kutta integration was performed in the "SORT" section. An inherent advantage of this section was the main feature of the CSMP; namely, the ability to identify internally in the program the sequence of computation steps so that a full dynamic interaction of the problem can be obtained. The programmer does not need to be concerned as to the sequence of program statements in this section; however, it will be noted in the program listing that a "people-oriented" sequence was used in order to make the program easier to read.

Output formatting was easily accomplished by identifying a "TITLE" plus a listing of variables of interest by a "PRINT" statement. Problem timing was established by the "TIMER" statement which specified the maximum (or finish) time, the problem time step increments and the output time printing step intervals. There were several numerical methods available for the integration scheme, with the choice depending upon the particular problem. This was specified by the "METHOD" statement. The "RANGE" statement provided a listing of the extremes, both minimum and maximum, for selected variables. Finally, the option was instituted of considering the problem as being completed (FINISH) when the fin-opening angle rate changed sign, which corresponded in a physical sense to the plastic collapse of the crushable stop prior to fin's blowing back about its pivot.

A program listing is provided in Appendix C in order to illustrate the readability (and hence simplicity) of the program. The FORTRAN statements in the main program were similar to usual techniques except that comment cards needed

an asterisk, * , in the first column in contrast to the "C" found in the subroutine section. In addition, the DIMENSION card required a virgule, / , in column 1 and continuation to a following card was indicated by ... at the end of the line. These distinctions are clearly explained in Ref. zz, hence the first-time user of CSMP should not experience great difficulty.

Some difficulty was encountered in setting up the time interval for the problem in order to maintain a balance between the fact that increasing the time step might degrade the time history solution accuracy and make the problem unstable and the other constraint that too small a time step interval could lead to computer time wastage. A problem time interval of 0.5 milliseconds was used at first, but it led to problem instabilities following the introduction of the crushable-stop logic into the program during the development period. A time step interval of 0.25 milliseconds worked quite well and avoided the above instability without requiring excessive computational time. In its final form, the program could provide a complete fin-opening dynamics solution in about six (6) seconds per condition, a time which was not considered excessive.

Output results will be found as a typical listing in Appendix C. The case shown is for an initial missile roll rate, P0(DY1 =), of 62.83 rad/sec and an initial fin-opening angle rate, P0(DY2 =), of 10.0 rad/sec. It will be clear from the listing that the fin opening process was stopped by the crushable-stop model at approximately 34 milliseconds for the specified condition. Computational results are discussed in the main body of this report.

```
*************************************************************************
*                                                                       *
*  ELASTIC-FIN OPENING DYNAMICS:  (8 INCH ERGP)                         *
*    INCLUDES FIN MODES: FIRST BENDING, FIRST TORSION                   *
*    INITIAL CONDITIONS: P0 = PHIDOT(0)                                 *
*                        T0 = THETADOT(0)                               *
*    GENERALIZED COORDS: Y1 = PHI                                       *
*                        Y2 = THETA                                     *
*                        Y3 = ALPHA                                     *
*                        Y4 = BETA                                      *
*                                                                       *
*************************************************************************
  INITIAL
/     DIMENSION A(4,4),B(4)
      CONSTANT AM=0.007591, AMB=0.001407, AMF=0.006184,  ...
               AI=0.859,  AI1=0.08742, AI2=0.09356, AI3=0.00633,  ...
               AI1F=0.05329, AI2F=0.05821, AI3F=0.00492,  ...
               R0=2.880, X1=-0.774, X3=5.225, DX3=4.731,  ...
               X1B=-0.140, X3B=0.801, X1F=-0.918, X3F=5.231,  ...
               FALPH=1.6813E+01, FBETA=5.1904E+04,  ...
               P0=62.832, P1=4.0E+04
      PARAMETER T0 = (0.0, 10.0, 20.0, 30.0, 40.0)
      FIXED I,J
      A1 = AI + 6.*AM*(R0**2)
      A2 = 6.*(AI1+AM*(X3**2))
      A3 = 6.*(AI3+AM*(X1**2))
      A4 = 3.*((AI1-AI3)+AM*((X3**2)-X1**2))
      A5 = 6.*((AMB*X1B*X3B)+(AMF*X1F*X3F))
      A6 = 6.*AM*R0*X1
      A7 = 6.*AM*R0*X3
      B1 = 6.*(AI2+AM*((X1**2)+X3**2))
      B2 = 6.*AMF*X1F*DX3
      B3 = 6.*AMF*X3F*DX3
      B4 = 6.*AMF*(DX3**2)
      B5 = 6.*AMF*R0*DX3
```

```
  DYNAMIC
NOSORT
      DO 1 I=1,4
      DO 1 J=1,4
    1 A(I,J) = 0.0
*   LOGIC FOR FIN CRUSHING THE STEEL STOPS
      IF(Y2.LT.1.047) GO TO 10
      IF(Y2.GT.1.047) GO TO 15
   10 AK=0.0
      GO TO 20
   15 AK=P1
   20 CONTINUE
      A(1,1) = A1 + A2*(SIN(Y2)**2) + A3*(COS(Y2)**2) + A5*SIN(2.*Y2) ...
               + 2.*A6*COS(Y2) + 2.*A7*SIN(Y2) + B4*(Y3**2)
      A(1,2) = (B3*COS(Y2) - B2*SIN(Y2))*Y3
      A(1,3) =-((6.*AI1F + B3)*SIN(Y2) + B5 + B2*COS(Y2))
      A(1,4) = 6.*AI3F*COS(Y2)
      A(2,1) = A(1,2)
      A(2,2) = B1
      A(3,1) = A(1,3)
      A(3,3) = 6.*AI1F + B4
      A(4,1) = A(1,4)
      A(4,4) = 6.*AI3F
      B12  =-(2.*A4*SIN(2.*Y2) + 2.*A5*COS(2.*Y2)  ...
             + 2.*A7*COS(Y2) - 2.*A6*SIN(Y2))
      B13  =-2.*B4*Y3
      B22  = (B2*COS(Y2) + B3*SIN(Y2))*Y3
      B23  = 6.*AI1F*COS(Y2)
      B24  = 6.*AI3F*SIN(Y2)
      G(1) = B12*DY1*DY2 + B13*DY1*DY3 + B22*(DY2**2) + B23*DY2*DY3 ...
             +B24*DY2*DY4
      C11  = (A4*SIN(2.*Y2) + A5*COS(2.*Y2) + A7*COS(Y2) - A6*SIN(Y2))
      C13  =-B23
      C14  =-B24
      G(2) = C11*(DY1**2) + C13*DY1*DY3 +C14*DY1*DY4
      G(2) = G(2) - AK
```

```
      D11   = B4*Y3
      D12   = ((6.*AI1F*DX3 + 2.*B3)*COS(Y2) - 2.*B2*SIN(Y2))
      F33   =-6.*FALPH
      G(3)  = D11*(DY1**2) + D12*DY1*DY2 + F33*Y3
      E12   = 6.*AI3F*SIN(Y2)
      F44   =-6.*FBETA
      G(4)  = E12*DY1*DY2 + F44*Y4
      CALL ELU(A,4,4)
      CALL SLVB(A,4,4,G)
SORT
      DY1   = INTGRL(P0,G(1))
      DY2   = INTGRL(T0,G(2))
      DY3   = INTGRL(0.,G(3))
      DY4   = INTGRL(0.,G(4))
      Y1    = INTGRL(0.,DY1)
      Y2    = INTGRL(0.,DY2)
      Y3    = INTGRL(0.,DY3)
      Y4    = INTGRL(0.,DY4)
TITLE       ELASTIC-FIN OPENING DYNAMICS: (8 IN. ERGP)
  PRINT     Y1,DY1,Y2,DY2,Y3,Y4
  RANGE     Y3,Y4
  METHOD    RKSFX
  TIMER     FINTIM = 0.200, PRDEL = 0.002, DELT = 2.50D-04
  FINISH    DY2 = -0.01
END
      P0 = 31.416
END
      P0 = 94.248
STOP
C*************************************************************************
C*                                                                       *
C*      SUBROUTINE SECTION FOLLOWS                                       *
C*  FOLLOWING TWO S/R'S SOLVE A SET OF SIMULTANEOUS LINEAR EQNS.         *
C*                                                                       *
C*************************************************************************
C ..
```

```
C .. ELU AND SLVB ARE A PACKAGE FOR SOLVING SETS OF SIMULT. EQNS.
C .. OF THE FORM:  A(N,N)*C(N) = B(N)
C .. AFTER SLVB USAGE, C(N) REPLACES B(N);
C .. N = ACTUAL MATRIX ORDER, ND = MAX. ORDER RESERVED IN PROGRAM
C ..
      SUBROUTINE ELU(A,N,ND)
      DIMENSION A(ND,ND)
      NM1=N-1
      DO 100 K=1,NM1
      KP1=K+1
      DO 100 I=KP1,N
      G=-A(I,K)/A(K,K)
      A(I,K)=G
      DO 100 J=KP1,N
  100 A(I,J)=A(I,J)+G*A(K,J)
      RETURN
      END
C ..
      SUBROUTINE SLVB(A,N,ND,B)
      DIMENSION A(ND,ND),B(ND)
      NM1=N-1
      NP1=N+1
      DO 100 K=1,NM1
      KP1=K+1
      DO 100 I=K 1,N
  100 B(I)=B(I)+A(I,K)*B(K)
      B(N)=B(N)/A(N,N)
      DO 300 K=2,N
      I=NP1-K
      J1=I+1
      DO 200 J=J1,N
  200 B(I)=B(I)-A(I,J)*B(J)
  300 B(I)=B(I)/A(I,I)
      RETURN
      END
ENDJOB
```

ELASTIC-FIN OPENING DYNAMICS: (8 IN. ERUP)

T0 = 10.000

TIME	Y1	DY1	Y2	DY2	Y3	Y4
0.0	0.0	62.832	0.0	10.000	0.0	0.0
2.0000D-03	0.1257	62.849	2.2059E-02	12.072	4.2103E-03	2.3177E-06
4.0000D-03	0.2514	62.817	4.8355E-02	14.244	1.0542E-02	8.5491E-06
6.0000D-03	0.3769	62.672	7.9139E-02	16.571	3.4591E-02	1.9003E-05
8.0000D-03	0.5019	62.355	0.1148	19.125	5.4095E-02	3.2991E-05
1.0000D-02	0.6262	61.841	0.1553	21.976	7.0352E-02	4.9057E-05
1.2000D-02	0.7492	61.143	0.2029	25.173	7.9836E-02	6.5572E-05
1.4000D-02	0.8707	60.317	0.2568	28.725	8.1300E-02	8.1434E-05
1.6000D-02	0.9904	59.436	0.3161	32.607	7.5280E-02	9.6959E-05
1.8000D-02	1.1084	58.571	0.3874	36.771	6.3504E-02	1.1375E-04
2.0000D-02	1.2247	57.744	0.4653	41.158	6.2564E-02	1.3498E-04
2.2000D-02	1.3394	56.909	0.5521	45.705	6.2179E-02	1.6335E-04
2.4000D-02	1.4522	55.943	0.6482	50.338	6.8606E-02	2.0143E-04
2.5000D-02	1.5629	54.578	0.7535	54.952	7.9779E-02	2.4443E-04
2.8000D-02	1.6707	53.008	0.8679	59.401	9.0593E-02	2.8479E-04
3.0000D-02	1.7747	50.958	0.9908	63.496	9.4500E-02	3.1234E-04
3.2000D-02	1.8745	48.854	1.1055	40.670	8.5647E-02	1.8915E-04
3.4000D-02	1.9703	47.022	1.1454	0.094	5.5905E-02	4.3430E-06
3.4250D-02	1.9820	46.844	1.1457	-4.995	5.0491E-02	-1.756E-05

$$$ SIMULATION HALTED FOR FINISH CONDITION DY2 -4.9947

RANGE OUTPUT BETWEEN 0.0 AND 3.4250D-02

VARIABLE	MINIMUM	TIME	MAXIMUM	TIME
Y3	0.0	0.0	9.4602E-02	2.9750E-02
Y4	-1.7558E-05	3.4250E-02	3.2027E-04	3.0750E-02

APPENDIX E

Estimation of Fin-Opening Rate:

The release of the fins by the fin latch when the ERGP leaves the gun barrel is dependent upon a relative velocity taking place between the latch and the missile fins. The relative motion occurs from several physical mechanisms including that the ERGP has a different deceleration manner than the fin latch block, possibly due to the latch block being totally immersed in the gun muzzle blast field immediately upon exiting from the barrel.

The latch is physically arranged to keep the fins locked in a folded position until the latch moves forward along the symmetry axis of the missile. A sketch of the configuration is shown on Fig. E-1 for sake of clarity. The forward motion of the latch is associated with a linear momentum, and it is the conversion of a portion of this linear momentum into fin angular momentum which may be considered as a source of the fin's initial opening angle rate.

The considerations which ensue are applications of momentum principles from enginnering mechanics such as described in Goldstein's text, Ref. 1. The fin latch has a "jump" or discontinuity in velocity (at time = $\emptyset$) due to the momentum transfer, and the velocity "jump" in combination with the latch's mass provides a measure of the momentum transfer. The time period involved in the momentum transfer is extremely short and the whole process may be considered somewhat in the manner of the application of a "Dirac delta" type of forcing function. The velocity "jump" is defined by:

$$\Delta V = [V(\emptyset+) - V(\emptyset-)] \qquad \ldots(E.1)$$

For purposes of the ensuing analysis, a unit value of velocity "jump" corresponding to one foot per second will be assumed in order to provide an estimate of fin-opening rate sensitivity. Pertinent dimensions for the development are shown on Fig. E-1 for sake of clarity, even though some are duplicated in Table I.

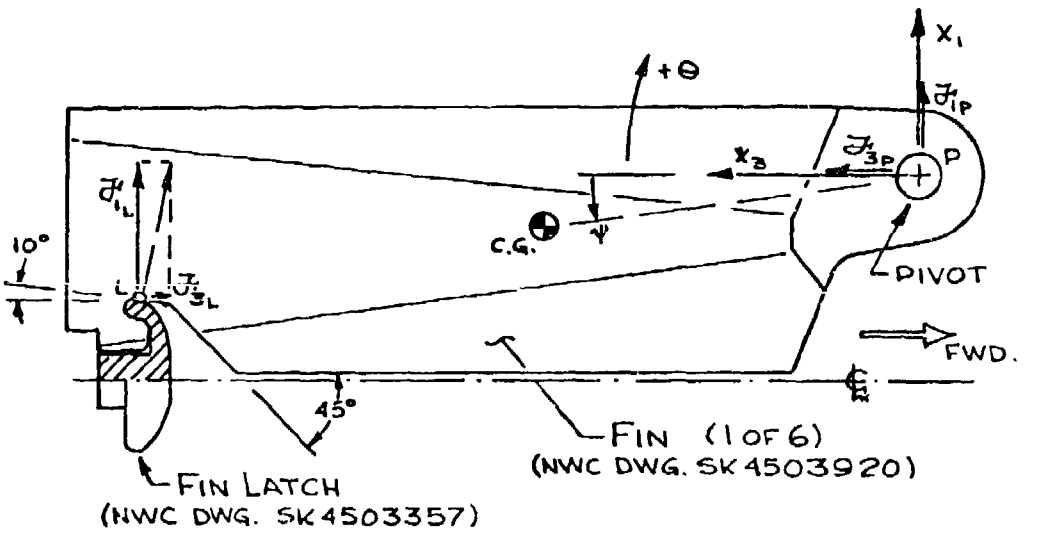

C.G. LOCATION

$X_1 = -0.774$ IN.

$X_3 = 5.225$ IN.

LATCH CONTACT

$X_{1_L} = -1.770$ IN.

$X_{3_L} = 11.00$ IN.

FIG. E-1: SKETCH OF FIN LATCH

It will be assumed that the impulse from the fin latch acts along the X_3 axis in the forward direction ($-X_3$). The radial impulse contribution is assumed to be reacting internal to the latch since all six fins share equally in the radial component. Therefore, the impulse at the latch contact point for one fin may be estimated as:

$$\mathcal{J}_{3_L} = \Delta I = (1/6)\, M_L \Delta V \qquad \ldots(\text{E.2})$$

$$= 0.003314 \text{ lb-sec}$$

where

W = weight of fin latch = 0.64 lb

M_L = mass of fin latch = 0.001657 lb-sec^2-in^{-1}

ΔV = velocity "jump" = 12 in-sec^{-1}

The radial contribution to the impulse transfer is based upon the true impulse acting normal to the fin trailing edge cutout with a 12 degree slope as sketched on Fig. E-1.

$$\mathcal{J}_{1_L} = \mathcal{J}_{3_L}/(\tan 12^\circ) = 0.01379 \text{ lb-sec} \qquad \ldots(\text{E.3})$$

In solving for the initial opening rate, three momentum conservation equations must be reconciled since an impulse reaction at the fin pivot is involved in the process.

Conservation of linear momentum (X_1 direction):

$$\mathcal{J}_{1_L} + \mathcal{J}_{1_P} - M \ell \cos\psi\, \dot{\theta}(0) = 0 \qquad \ldots(\text{E.4})$$

Conservation of linear momentum (X_3 direction):

$$\mathcal{J}_{3_L} - \mathcal{J}_{3_P} + M \ell \sin\psi\, \dot{\theta}(0) = 0 \qquad \ldots(\text{E.5})$$

Conservation of angular momentum (about fin c.g.):

$$I_2 \dot{\theta}(0) = \mathcal{J}_{1_L}(X_{3_L} - X_3) - \mathcal{J}_{1_P}(X_3) + \mathcal{J}_{3_L}(X_{1_L} - X_1) + \mathcal{J}_{3_P}(X_1) \qquad \ldots(\text{E.6})$$

In the above conservation expressions, it is recognized that:

W = fin weight = 2.93 lbs

M = mass of a fin = 0.007591 lb-sec^2-in^{-1}

I_2 = fin mass moment of inertia component about the c.g. = 0.09358 lb-in-sec^2

$\ell = (X_1^2 + X_3^2)^{1/2}$ = 5.252 in.

$\sin\psi$ = 0.1465

$\cos\psi$ = 0.9892

Substituting numerical values into eqns. E.4 through E.6 yields:

$$\mathcal{J}_{1P} - 0.03966\,\dot{\Theta}(0) = -0.01679 \text{ lb-sec}$$

$$\mathcal{J}_{3P} - 0.00587\,\dot{\Theta}(0) = +0.00331 \text{ lb-sec}$$

$$5.225\,\mathcal{J}_{1P} + 0.774\,\mathcal{J}_{3P} + 0.09358\,\dot{\Theta}(0) = +0.10521 \text{ lb-sec}$$

Finally, the numerical solution for initial fin opening angle rate becomes:

$$\dot{\Theta}(0) = 0.658 \text{ rad-sec}^{-1} \qquad \ldots(\text{ E.7 })$$

which is a result of an impulse input from the fin latch due to a unit velocity "jump" of one foot per second.

REFERENCES

1. Goldstein, H., Classical Mechanics, Addison-Wesley, 1950.

2. ---, "Trailing Fin", NWC Dwg. SK4503920, 10 March 1977.

3. Speckhart, F.H. and Green, W.L., A Guide to Using CSMP-The Continuous System Modeling Program, Prentice-Hall, 1976.

4. Payne, H., Private Communication of SAP IV Structural Input Data Cards, 12 May 1977.

5. Bathe, K.J., Wilson, E.L. and Peterson, F.E., "SAP IV, A Structural Analysis Program for Static and Dynamic Response of Linear Systems", UCLA Rep. EERC 73-11, April 1974.

6. ---, "Wedge Fin", NWC Dwg. SK4503332, 23 July 1976.

7. Purcell, N., "8-in. ERGP Fin Load and Stress Analysis", NWC Memo 3273/NLP:km, 10 August 1977.

8. Boone, J.N., "A Consistent Formulation of the Fin Deployment Problem", NSWC/DL Rep. TR-3736, October 1977.

DISTRIBUTION LIST

		No. Copies
1.	Library Code 0142 Naval Postgraduate School Monterey, CA 93940	2
2.	Defense Documentation Center Cameron Station Alexandria, VA 22314	2
3.	Department of Aeronautics Code 67 Naval Postgraduate School Monterey, CA 93940 M.F. Platzer, Chairman (1) L.V. Schmidt, Professor (10)	11
4.	Dean of Research Code 012 Naval Postgraduate School Monterey, CA 93940	1
5.	Commanding Officer Naval Air Systems Command Washington, D.C. 20361 Attn: AIR-954	2
6.	Commanding Officer Naval Sea Systems Command Washington, D.C. 20362 Attn: SEA-09B32	2
7.	Commanding Officer Naval Ordnance Station Indian Head, MD 20640 Attn: Code 5232 (1) Code 5232E (1)	2
8.	Commanding Officer Naval Surface Weapons Center, Dahlgren Laboratory Dahlgren, VA 22448 Attn: Code G-20 (1) Code G-21 (5) Code G-30 (3) Code N-41 (1)	10

		No. Copies
9.	Commanding Officer Naval Weapons Center China Lake, CA 93555 Attn: Code 003 (1) Code 01 (1) Code 03A (1) Code 23 (1) Code 233 (4); 3 plus archives copy Code 2336 (1) Code 31 (1) Code 3161 (2) Code 32 (1) Code 3204 (1) Code 324 (1) Code 326 (1) Code 327 (1) Code 32703 (1) Code 3271 (1) Code 3272 (1) Code 3273 (10) Code 3274 (5) Code 3275 (1) Code 3276 (1) Code 33 (1) Code 35 (1) Code 36 (1) Code 3586 (1); B. Ford Code 38 (1) Code 39 (1) Code 6211 (1) Code 6212 (1)	45
10.	Navy GP Technical Representative Office c/o Martin-Marietta Corporation Orlando, FL 32855 Attn: Code MP-354	1